2

UDR-TR-92-72

DETERMINATION OF THE DYNAMIC UNLOAD/RELOAD CHARACTERISTICS OF CERAMICS

BY:

G. ABFALTER
N.S. BRAR
D. JURICK

JUNE 1992

U.S. ARMY RESEARCH OFFICE

CONTRACT NO.: DAAL03-88-K-0203

UNIVERSITY OF DAYTON
RESEARCH INSTITUTE
DAYTON, OHIO 45469-0180

The University of Dayton

REPORT DOCUMENTATION PAGE

Form Approved
OMB No 0704-0188

1. AGENCY USE ONLY *(Leave blank)*

2. REPORT DATE
June 1992

3. REPORT TYPE AND DATES COVERED
Final Report -- Oct 1988 - March 1992

4. TITLE AND SUBTITLE
Determination of the Dynamic Unload/Reload Characteristics of Ceramics

5. FUNDING NUMBERS
DAAL03-88-K-0203

6. AUTHOR(S)
G. Abfalter, N. Brar, D. Jurick

7. PERFORMING ORGANIZATION NAME(S) AND ADDRESS(ES)
University of Dayton Research Institute
300 College Park
Dayton, OH 45469-0180

8. PERFORMING ORGANIZATION REPORT NUMBER
UDR-TR-92-72

9. SPONSORING/MONITORING AGENCY NAME(S) AND ADDRESS(ES)
U. S. Army Research Office
P. O. Box 12211
Research Triangle Park, NC 27709-2211

10. SPONSORING/MONITORING AGENCY REPORT NUMBER
ARO 26169.11-MS-A

11. SUPPLEMENTARY NOTES
The view, opinions and/or findings contained in this report are those of the author(s) and should not be construed as an official Department of the Army position, policy, or decision, unless so designated by other documentation.

12a. DISTRIBUTION/AVAILABILITY STATEMENT
Approved for public release; distribution unlimited.

12b. DISTRIBUTION CODE

13. ABSTRACT *(Maximum 200 words)*

Ballistic impacts on ceramics give rise to many complex phenomena. Common features of many aspects of target response include compressive failure, followed by shear and/or tensile failure, followed by bulk motion (flow) of damaged material. As a leader in both shock physics and terminal ballistic research, the University of Dayton Research Institute (UDRI) performed the study of the behavior of ceramics subjected to these unusual loading conditions which is the subject of this report.

To investigate these phenomena we developed, modified, and/or improved a set of impact tests to exercise ceramics in stress states and stress histories that are characteristic of ballistic impact. This set included the transverse gauge technique, bar impacts, reverberation technique, unload/reload technique, etc. We used these experiments to gain insight into the behavior of ballistic ceramics important to DARPA research groups. Included in the ceramics studied were TiB_2 B_4C, AlN.

We developed correlations, based upon empirical data, between the material properties and the ballistic properties of ceramics. The correlations included the
(continued on reverse)

14. SUBJECT TERMS
Long rod penetrators, armor, ceramic armor, ballistic testing, plate impact, shock loading, penetration studies, ceramics, .50 cal SLAP, projectiles, glass, brittle materials

15. NUMBER OF PAGES
53

16. PRICE CODE

17. SECURITY CLASSIFICATION OF REPORT	18. SECURITY CLASSIFICATION OF THIS PAGE	19. SECURITY CLASSIFICATION OF ABSTRACT	20. LIMITATION OF ABSTRACT
UNCLASSIFIED	UNCLASSIFIED	UNCLASSIFIED	UL

13. ABSTRACT (Concluded)

relation of Tate target strength (R_t) to the Hugoniot elastic limit (HEL) and the relation of the loss of shear strength to the ballistic performance of brittle solids.

We determined the dynamic material properties and performed ballistic testing on proprietary cermaics supplied to ARO by several ceramic research groups and manufacturers.

The principal investigator, Dr. Stephan Bless, created and maintained open communication with the other DARPA research groups supplying them with data, and analysis, and performing tests and experiments for them. Dr. Bless was a very active participant at all DARPA, ARP and BTI topical meetings of consequence. He chaired the committee for developing a ceramic screening test methodology. UDRI organized, hosted, and chaired an ARO-sponsored meeting on 18 April 1989 to discuss ceramic screening tests.

This short synopsis shows that we more than adequately complied with the requirements of the statement of work.

TABLE OF CONTENTS

TABLE OF CONTENTS
(Continued)

LIST OF FIGURES

LIST OF TABLES

FOREWARD

Dr. Stephan J. Bless was the principle investigator responsible for the conduct of this effort until his departure from the University in August 1991. In September 1991, Mr. Garry H. Abfalter assumed responsibility and completed the effort as principal investigator. Dr. Nachatter S. Brar contributed significantly to the effort by conducting many experiments and documenting the results and findings in numerous technical papers and presentations. Messrs. Bechara Azzi and Donald Jurick provided invaluable assistance to Dr. Brar, Dr. Bless, and Mr. Abfalter in completion of the technical analysis and documentation produced under this contract.

The principal investigators thank Dr. Kalaisam Iyer and Dr. Iqbal Ahmad, the technical monitors, for their technical guidance and direction during the performance of this contract.

Other reports and papers generated through this contract are identified in the list of references included in Section 1.

SUMMARY

Ballistic impacts on ceramics give rise to many complex phenomena. Common features of many aspects of target response include compressive failure, followed by shear and/or tensile failure, followed by bulk motion (flow) of damaged material. As a leader in both shock physics and terminal ballistic research, the University of Dayton Research Institute (UDRI) was uniquely qualified to perform the study of the behavior of ceramics subjected to these unusual loading conditions which is the subject of this report.

To investigate these phenomena we developed, modified, and/or improved a set of impact tests to exercise ceramics in stress states and stress histories that are characteristic of ballistic impact. This set included the transverse gauge technique[2], bar impacts [3,5], reverberation technique[4], unload/reload technique[6], etc. We used these experiments to gain insight into the behavior of ballistic ceramics important to DARPA research groups. Included in the ceramics studied were TiB_2, B_4C[8,12], AlN[7,9,11].

We developed correlation's, based upon empirical data, between the material properties and the ballistic properties of ceramics. The correlations included the relation of Tate target strength (R_t) to the Hugoniot elastic limit (HEL)[1] and the relation of the loss of shear strength to the ballistic performance of brittle solids[10].

We determined the dynamic material properties and performed ballistic testing on proprietary ceramics supplied to ARO by several ceramic research groups and manufacturers.

The principal investigator, Dr. Stephan Bless, created and maintained open communication with the other DARPA research groups supplying them with data, and analysis, and performing tests and experiments for them. Dr. Bless was a very active participant at all DARPA, ARO, and BTI topical meetings of consequence. He chaired the committee for developing a ceramic screening test methodology. UDRI organized, hosted, and chaired an ARO-sponsored meeting on 18 April 1989 to discuss ceramic screening tests.

This short synopsis shows that we more than adequately complied with the requirements of the statement of work.

SECTION 1
PRIMARY RESULTS AND FINDINGS

1. SPECIFIC ATTAINMENTS

In order to study the dynamic behavior of ceramics we developed, modified, and/or improved the following impact experiment techniques:

- shock-reshock
- shock-reload
- shock-unload-shock
- direct measurement of strength
- effect of pressure and strain rate
- propagation of failure waves

Under our direction, RDA developed damage-accumulation and constitutive models by simulating plate and bar impact experiments. We developed a three dimensional, continuum mechanics based, ceramic constitutive model[13].

Alternative methods for ceramic screening were also developed. It was proposed and advocated that ballistic resistance rather than differential mass efficiency be used to characterize ceramic performance[14].

2. DYNAMIC CHARACTERIZATION OF CERAMICS

UDRI determined the dynamic behavior of several ceramics using various experimental techniques. The advanced ceramics investigated included AlN, B_4C, and TiB_2.

The dynamic response of AlN was determined in a series of plate impact experiments using manganin gauges both in the longitudinal and lateral orientations to the shock direction[7,9,11]. The shear strength of the shocked material beyond its HEL was determined, thus, demonstrating the value of the development of the transverse gauge technique.

Dynamic properties of B_4C were also measured. The results were compared with the theoretical predictions of various models[8,12,15].

A double impact technique was developed and used to determine the strength of shock loaded ceramics. A quantitative measure of the damage induced by low amplitude shock waves was obtained[16].

Recent experimental developments to study the dynamic response of ceramics to impulsive loading were reviewed. These included: (1) the transverse gauge configuration, (2) double flyer plate techniques, and (3) the bar impact configuration to measure yield strength under 1-d stress conditions[17].

Researchers used a reverberation technique to study the load/unload behavior of TiB_2, AlN and B_4C[4].

The strength of TiB_2 was measured under shock compression and after step unloading by using transverse manganin gauges. The pressure hardening exhibited by the material was conjectured to explain its superior ballistic performance[2].

3. GLASS AS A BRITTLE MATERIAL

The reverberation plate technique was applied to soda lime glass to see if the dynamic unloading behavior of brittle materials could be determined. The unloading behavior observed was similar to that of quartz giving strong indication that the technique is viable[20].

Experiments were conducted to determine the spall strength of soda lime glass. Additional experiments were conducted to monitor the existence of a fracture wave propagating away from the impact zone behind which the spall strength is zero[21].

4. FAILURE WAVES IN GLASS

We performed both plate impact and bar impact experiments on soda lime glass and pyrex to investigate failure waves. Failure waves were observed to propagate behind the compression waves. The material traversed by the failure wave suffers a total loss of tensile strength and a substantial drop in shear strength. The results of these extensive experiments were reported in several publications[22-25].

5. BAR IMPACT EXPERIMENTS

The failure of ceramics and glass was studied with instrumented bars and an IMACON high speed framing camera[3,5]. UDRI's ceramic constitutive model, based on 3-d continuum mechanics, was used to model AD-85 ceramic. The AD-85 model was employed in the finite element computer program, EPIC-2, to model a symmetric rod impact[13].

6. CORRELATION OF MATERIAL PROPERTIES AND BALLISTIC PERFORMANCE

An understanding of "Tate target strength", R_t, as a general property of ceramics that can be derived from screening tests was developed[18]. Its use as a single parameter for describing the penetration resistance of ceramics was derived. The value of R_t was shown to be closely correlated with the HEL of ceramics[1].

Ballistic experiments demonstrated a correlation between loss of shear strength of shock loaded brittle solids; soda lime glass and alumina; and decreased ballistic penetration resistance[10].

Analysis of the ballistic efficiency of alumina and sapphire revealed that good ballistic resistance correlates much better with shock strength than with fracture toughness[19].

7. DEPTH-OF-PENETRATION EXPERIMENTS

There is a continuing need for government and industrial laboratories to efficiently evaluate new ballistic materials. A primary means of evaluating such materials is the depth-of-penetration (DOP) test[26] and described in Section 2.

We evaluated and screened advanced ceramics for ballistic performance using the DOP technique for other ARO contractors and members of the DARPA/BTI program, particularly for Dow Chemical, Georgia Tech Research Institute, and SUNY-Buffalo. The results of this testing is reported in the attached documents.

During the course of the program a large DOP data base was developed. We recommend that a follow-on program be initiated to use statistical methods to analyze these data.

8. COMMUNICATION WITH OTHER DARPA RESEARCH GROUPS

Throughout the program, UDRI engaged in frequent communication and data interchange with other DARPA research groups. Dr. Bless was an active participant in the

Los Alamos Scientific Laboratories (LASL) Ceramics Working Group. He presented a synopsis of UDRI modeling of ceramic armor and interpretation of the Phermex data at their 6 and 7 December 1989 meeting. He presented early bar impact results at the 10 March 1989 meeting. At this meeting Dr. A.M. Rajendran presented UDRI's ceramic failure model.

Dr. Bless chaired an ARO Committee to develop a standardized ceramic screening methodology. UDRI organized, hosted, and chaired an ARO-sponsored meeting on 18 April 1989 to discuss ceramic screening tests. Dr. Bless was the driving force behind and prepared the Draft Summary of Findings of the Committee on Standardization of the Test Methodology for Ballistic Performance of Ceramics and Cermets.

Stephan Bless was an active participant in the 4 December 1989 BTI Advanced Computational Methods Progress Review and BTI Advanced Armor/Anti-Armor Materials Program Progress Review. Mr. Abfalter, Dr. Bless, and Stephen Hanchak participated in the TACOM sponsored meeting on "Impact Test Methods for Characterization of Ceramic Materials for Armor Components" on 17-18 December 1991 held at the Jet Proposal Laboratory.

9. CONCLUSIONS

During the course of this program UDRI developed, improved, and/or modified a number of impact experiments. These and other techniques were used to develop material and ballistic properties of ceramics of current interest to ARO and DARPA. Our analysis determined correlations between ceramic material properties and ballistic performance. We performed DOP testing, evaluation and consulting for other members of the DARPA research community. We established and maintained excellent communications and working arrangements with the other members of the DARPA research community. We took a leadership role in many areas, e.g., the development of a standardized ceramic screening test methodology. We advanced the state of the art in the testing of ceramics and immensely broaden the knowledge of the dynamic behavior of ceramics and brittle materials.

10. RECOMMENDATIONS

The DOP data base developed during this program may contain more information than currently reported. Sophisticated statistical techniques may yield correlations between ballistic properties of ceramics and other properties. They might also point the direction for future testing to rationally fill out the data base to answer open questions on such correlations.

SECTION 1
REFERENCES

1. Z. Rosenberg, S.J. Bless, Y. Yeshurun, and N.S. Brar, "On the Relation Between the Penetration Resistance of Ceramics and Their Dynamic Properties," Proceedings, 6th International Conference on Mechanical Behavior of Material, ICM 6, 29 July - 2 August 1991, Kyoto, Japan, Pergamon Press, 1991.

2. Z. Rosenberg, N.S. Brar, and S.J. Bless, "Shear Strength of Titanium Diboride Under Shock Loading as Measured by Transverse Manganin Gauges," Proc. APS 1991 Topical Conf. Shock Compression Condensed Matter, ed. S.C. Schmidt et al., Elsevier, 199[illegible].

3. N.S. Brar and S.J. Bless, "Dynamic Fracture and Failure Mechanisms of Ceramic Bars," International Conference on Shock-Wave and High-Strain Rate Phenomena in Materals (Explomet 90), San Diego, CA, 12-17 August 1990.

4. S.J. Bless and N.S. Brar "Load/Unload Hysteresis in Ceramics Measured By A Reverberation Technique," Proc. APS 1991 Topical Conf. Shock Compression Condensed Matter, ed. S.C. Schmidt et al., Elsevier, 1992.

5. S.J. Bless, N.S. Brar, and Z. Rosenberg, "Failure of Ceramic and Glass Rods Under Dynamic Compression," in Shock Compression of Condensed Matter, 1989, eds. S.C. Schmidt, et al., p 939-942, Elsevier Science Publishers, 1990.

6. S. Bless, M. Alme, N. Brar, and A. Rajendran, "Determination of Unload/Reload Properties of Ceramics," DoD/DARPA Coordinating Meeting on Advanced Armor/Anti-Armor Materials and Advanced Computational Methods, Radisson Mark Plaza Hotel, Alexandria, VA, 13-15 December 1988.

7. Z. Rosenberg, N.S. Brar, and S.J. Bless, "Dynamic High-Pressure Properties of AlN Ceramic as Determined By Flyer Plate Impact," J. Appl. Phys. **70** (1), July 1991.

8. N.S. Brar, Z. Rosenberg, and S.J. Bless, "Shock Hugoniot of Porous and Fully Dense B_4C," submitted to Topical Conference Shock Compression of Condensed Matter, June 1991.

9. N.S. Brar, S.J. Bless, and Z. Rosenberg, "Response of Shock-Loaded AlN Ceramics Determined with In-Material Manganin Gauges," International Conference on Shock-Wave and High-Strain Rate Phenomena in Materials (Explomet 90), San Diego, CA, 12-17 August 1990.

10. Z. Rosenberg, S.J. Bless, and N.S. Brar, "On the Influence of the Loss of Shear Strength on the Ballistic Performance of Brittle Solids," Int'l. J. Engng., 9:45-50, 1990.

SECTION 1
REFERENCES
(Continued)

11. Z. Rosenberg, N.S. Brar, and S.J. Bless, "The Dynamic Response of AlN," final technical report, UDR-TR-89-74, June 1990.

12. N.S. Brar, and Z. Rosenberg, and S.J. Bless, "Dynamic Properties of Porous B_4C," interim report, UDR-TM-89-15, January 1990.

13. D. J. Grove, A. M. Rajendran, E. Bar-On, and N. S. Brar, "Damage Evolution in a Ceramic Rod," 1991 Topical Conference on Shock Compression of Condensed Matter, Williamsburg, Virginia, 17-20 June 1991.

14. S.J. Bless and M. Alme, "A Fresh Approach to Analyzing Ceramic Screening", internal report.

15. Z. Rosenberg, N.S. Brar, and S.J. Bless, "Applying Steinberg's Model to the Hugoniot Elastic Limit of Porous Boron Carbide Specimens," Proc. APS 1991 Topical Conf. Shock Compression Condensed Matter, ed. S.C. Schmidt et al., Elsevier, 1992.

16. Z. Rosenberg, N.S. Brar, and S.J. Bless, "Determination of the Strength of Shock Loaded Ceramics Using Double Impact Techniques," Shock Compression of Condensed Matterd-1989, Elsevier, 1990.

17. N.S. Brar, S.J. Bless, and Z. Rosenberg, "Response of Shock-Loaded AlN Ceramics Determined with In-Material Manganin Gauges," International Conference on Shock-Wave and High-Strain Rate Phenomena in Materials (Explomet 90), San Diego, CA, 12-17 August 1990.

18. S.J. Bless and M. Alme, "Use of Tate Theory to Describe Penetration of Thick Ceramics," Sixth TACOM Armor Coordinating Conference, Gaithersburg, MD, April 1990.

19. N. S. Brar, S. J. Bless, and Z. Rosenberg, "Factors Affecting Ballistic Efficiency of Alumina and Sapphire," 1989 Topical Conference on Shock Compression of Condensed Matter, Albuquerque, New Mexico, 14-17 August 1989.

20. C. Lopatin, S. J. Bless, and N. S. Brar, "Dynamic Unloading Behavior of Soda Lime Glass and Titanium Diboride," 1989 Topical Conference on Shock Compression of Condensed Matter, Albuquerque, New Mexico, 14-17 August 1989.

21. N.S. Brar, Z. Rosenberg, and S.J. Bless, "More on the Spall Strength of Shock Loaded Glass," 3e Congres International sur le Comportement Mechanique et Physique des Materiaux sous Sollicitations Dynamiques, Strasbourg, October 1991.

SECTION 1
REFERENCES
(Concluded)

22. N. S. Brar, Z. Rosenberg, and S. J. Bless, "Spall Strength and Failure Waves in Glass," 3e Congres International sur le Comportement Mechanique et Physique des Materiaux sous Sollicitations Dynamiques, Strasbourg, October 1991.

23. N. S. Brar, S. J. Bless, and Z. Rosenberg, "Impact Induced Failure Waves in Glass Bars and Plates," Appl. Phys. Letters, 59, 3396-3398 (1991).

24. S.J. Bless, N.S. Brar, G.I. Kanel, and Z. Rosenberg, "Failure Waves in Glass," J. American Ceramics Society, May 1992 (to be published).

25. N.S. Brar and S.J. Bless, "Failure Waves in Glass Under Dynamic Compression," presented at the Satellite Conference of the XIII AIRAPT International Conference on High Pressure Science and Technology held at BARC Bombay, India, 14-15 October 1991.

26. S. Bless and N. Brar, "Comparative Evaluation of Ceramics with .50 SLAP Penetrator," UDR-TR-91-110, Internal Report, Contract No. DAAL03-88-K-0203, August 1991.

SECTION 2

COMPARATIVE EVALUATIONS OF CERAMICS WITH .50 SLAP PENETRATOR

1. BACKGROUND

Work reported herein was sponsored by the U.S. Army Research Office (ARO) and by Dow Chemical Corporation. The Project Manager for ARO was Dr. Kailasam Iyer. The Project Manager for Dow was Dr. William Rafaniello. Hot-pressed TiB_2/Al_2O_3 samples were provided by Georgia Tech Research Institute (GTRI). Kathryn Logan was the Project Manager for GTRI. One each sintered AlN tile and a sintered TiB_2 composite tile were supplied by Dr. Vladmir Hlvacek of the State University of New York at Buffalo (SUNY-B). Experiments were conducted in the facilities of the University of Dayton Research Institute Impact Physics Laboratory. Range Technicians Stephen Hanchak and Thomas Williams are to be commended for their support in assembling targets and performing ballistic tests for this effort. This report constitutes a final topical report.

A. Armor Ceramics

Future fighting vehicles will be required to survive impacts by advanced projectiles that have greater penetration ability than current threats. However, these vehicles will have little or no increased weight allowance for armor. Consequently, new armor designs will be required that provide greater weight efficiency. It is quite likely that the performance goals of new armor will require use of ceramics[1].

There have been many experimental programs that have demonstrated superior performance of armor targets that include advanced ceramic tiles. Unfortunately, it has usually been found that top level performance is only achieved using fully dense AlN, TiB_2, or SiC made by relatively expensive hot pressing techniques.

Under ARO sponsorship, several alternative processing schemes have been investigated that may lead to much less expensive armor-grade ceramics. Dow Chemical developed new processing techniques to produce sintered AlN and AlN/SiC composites. GTRI and the SUNY-B developed reaction sintered TiB_2 and TiB_2 composites.

B. DOP Test Technique

There is a continuing need for government and industrial laboratories to efficiently evaluate new ballistic materials. One of the main ways that this can be done is by means of depth of penetration (DOP) tests.

In a DOP test, the test material is placed onto a substrate of a reference material. The projectile is designed so that it will penetrate the test materials and come to rest after penetration, P_R, in the substrate. This type of testing was first used to derive performance criteria for ceramics in the mid 1980's[2,3,4]. It has since come into widespread use[5,6,7].

There are several ways to analyze DOP results. A common technique is to compute the differential efficiency of the test material with respect to the substrate. The formula for this is:

$$\Delta e_m = \frac{W_{REF} - W_R}{W_C}$$

Here, W_{REF} is the areal density of the substrate that would be penetrated if there were no armor material, W_R is the areal density of the substrate penetrated below the armor material, and W_C is the areal density of the armor material. For example, if $\Delta e_m = 2$, then the armor material provides a given level of protection at half the weight of the substrate.

Another analysis technique to compute the performance of a test material relative to a reference material is

$$e_{REL} = \left[\frac{W_{REFMATL}}{W_C}\right]_{\text{same } P_R}$$

As with Δe_m, the tested ceramic provides the same protection as the reference material at $1/e_{REL}$ times the weight of the reference material. The reference material of interest is usually RHA (rolled homogeneous armor, MIL-SPEC-12560).

A variety of different geometries have been used to perform DOP tests. In order to resolve discrepancies, ARO formed a committee in 1989 to propose standard techniques for conducting DOP tests. The committee made a set of recommendations which are summarized in Exhibit 1.1. These have not yet been formally acted on by the government. However, they have been closely adhered to in the current work.

The most significant modification to the protocol in Exhibit 1.1 was the replacement of the .50 M2AP bullet by the .50 Olin SLAP (sabot light armor piercing) bullet. The motivation for this substitution was that the intended application of the tested ceramics is for heavy armor. Heavy armor threats are generally long rods made from tungsten or uranium alloys. The stress levels produced on impact are of the order $\sigma_0 = 1/2\ \rho_P V_S^2 + Y_P$ (where ρ_p is penetrator density, V_S is impact velocity, and Y_P is penetrator strength). For typical impact velocities of 1.5 to 1.7 km/s, $220 < \sigma_0 < 280$ kbar. These stresses are considerably more than those produced by impact of a .50 M2AP, for which $\sigma_0 \approx 50$ kbar. Moreover, long rods are defeated by erosion within the tile, whereas M2AP bullets are generally defeated by shatter on the tile surface. The impact dynamics of the LRP are more nearly simulated by the SLAP bullet. For the SLAP, $\sigma_0 = 150$ kbar. Moreover, like the LRP, the SLAP is defeated by erosion.

2. TEST METHODOLOGY AND REFERENCE DATA

A. Launch

The projectiles used in this study were manufactured Olin Corporation, and are designated .50 caliber SLAP . A subcaliber penetrator is carried by a separating sabot. The base of the penetrator is keyed by a slot to an aluminum pusher in the sabot so that the penetrator is spin stabilized by the action of the barrel rifling grooves. The projectiles were shot as received, using a 1:15 twist rate barrel that was 1.05 m long (UDRI S/N-0528). The average velocity that was obtained was 1215 m/s and the standard deviation was 10 m/s.

B. Projectile

The penetrator material is 95 percent W-Ni-Fe. The diameter is 7.72 mm and the mass is 23.2 g. It is pictured in Figure 2.1. The mechanical properties of the SLAP alloy were recently measured on our split Hopkinson bar. Figure 2.2 illustrate a typical stress strain curve[8]. The compressive strength is about 20 kbar (2 GPa).

C. Targets

The round ceramic tiles were embedded in round 6061-T6 aluminum bars that were at least 25 mm larger in diameter than the tiles. Cavities were machined into the aluminum to hold the ceramic target discs. Each cavity for the ceramic was machined individually to allow a good slip fit. The ceramics were glued in place using 5-minute epoxy. The bond lines on the base of the ceramic were less than or equal to 0.25 mm thick. Except for a few cases, noted in the shot matrix, the thickness of aluminum below the ceramic was approximately 125 mm.

D. Reference Data

The penetration of this projectile into 6061T651 aluminum was measured to be 210 mm (shot 9-3226). The penetration is so large in aluminum because the projectile tip does not deform. A more useful reference number perhaps is the penetration of a round-nose 21 g version of the SLAP projectile. This was an average of 130 mm (shots 9-2668 and 2669).

3. RESULTS

Table 2.1 shows the DOP test matrix. The columns in this table contain the following information:

A: Reference number

B: Material identification

C: Tile diameter or width, (mm)

D: Tile shape, Round or Square

E: Tile thickness, (mm)

F: Tile mass, (gr)

G: Tile density, (g/cm^3)

H: Tile areal density, W_C (g/cm^2)

I: Shot number (on our Range 9)

J: Velocity, (m/sec)

K: Penetration, P_r (mm)

L: Aluminum backing length, S is 100 mm, otherwise > 125 mm (other notes in text)

M: Sponsorship, D denotes Dow tiles, G denotes GTRI tiles, SUNY denotes SUNY-B, otherwise ARO

Initially 100 mm thick aluminum blocks were used as backing material. However, in some shots there was bulging of the rear surface. In order to prevent this we switched to 125 mm or longer aluminum blocks. The shots in which the rear surface of the substrate bulged may be less reliable and they are noted "S, B" in column L and with B in Figure 2.6.

Figures 2.3 and 2.4 are photographs that show most of the radiographs of penetration cavities. It can be seen that there is a tendency that when the penetration is shallow, there is often an early side spur, suggesting that the projectile split passing through the tile. Cavity diameters can also be measured from the radiographs. However, there was very little correlation between cavity diameter and penetration depth.

Most of the original series of tiles tested had an areal density 3 ± 0.01 g/cm², so the depths of penetrations can be directly compared. This is shown in Figure 2.5. For reference, Carborundum sintered SiC, AD995 (from interpolation, on line between two data points), and TiB_2 data are also included. It should be noted that the Carborundum SiC tiles were 6 x 6 inch. The larger size may have a small effect on performance. The TiB_2 tiles were either 3 x 3 or 4 x 4 inch and unconfined. TiB_2 tiles of these sizes did not differ in performance.

The effect of tile shape was examined by testing two square shaped tiles of sintered AlN. These are noted SQ in column D of Table 2.1 and in Figure 2.6. The two 4-inch square AlN tiles yielded an average penetration of 63.8 mm. This is 5.6 mm below the average for round AlN tile penetration. Thus it is probable that the DOP values of square AlN tiles would be a little lower than the DOP values of round AlN tiles.

The ceramics clearly rank as groups. The sintered AlN materials are less effective than the AlN/SiC hot pressed composites, which are a little less effective than the sintered SiC materials. Within a class of material there are only small differences. Correlations between performance and composition will probably be discussed in a separate report by Dow. Figure 2.6 shows the penetration by ceramic groups. According to Dow, Materials 36, C, N and SD are all standard AlN composition from different batches. There were two grain distributions among the AlN/SiC mixtures. There was not a significant difference in the performance of these two types of materials.

The best sintered AlN, Material 29, had the highest compression strength of the AlN's. It also performed best in a previous study with .30 M2AP bullets (ballistic limit tests).

There is appreciable scatter in these DOP results. Deeper penetration appears to occur when the projectile remains intact passing through the ceramic.

A sintered AlN and a TiB_2 composite provided by SUNY-B were also evaluated. The TiB_2 composite defeated the projectile at an areal density of 6.26 g/cm². An additional set of AlN/SiC tiles (100 mm diameter) were evaluated late in the program for Dow. The tiles (Reference Nos. 70 through 85) varied in composition to provide areal densities from 4.22 to 7.35 g/cm². Materials Reference Nos. 77, 78, 79, and 81 performed exceptionally well as shown in Figure 2.7.

4. CONCLUSIONS

Overall, no new material tested in this program performed better than conventional sintered SiC. However, many materials performed as well or better than AD995, which is the current state-of-the-art sintered alumina. If these materials can be made for reduced cost, then they have much merit as potential armor materials.

The results described here cannot be reliably extrapolated to other threat categories. In particular, different results might be obtained with brittle bullets (such as steel AP bullets or WC bullets) or with long rod penetrators.

To firm the conclusions and gain additional insight from the data, it is recommended that statistical techniques be applied to the data base. Statistical analysis should also give direction to completing the data base and answering open questions.

TABLE 2.1. ARO TEST MATRIX

A	B	C	D	E	F	G	H	I	J	K	L	M
Ref. No.	Tile Material Identification	Tile Dia. (mm)	Tile Shape	Tile Thck (mm)	Tile Mass (gr)	Tile Dens. (g/cm^3)	A.D. (g/cm^2)	Shot No.	Velocity (m/s)	Pr (mm)	Al Length	Sponsor
1	AIN (1-2A)	99.03	R	8.84	230.3	3.400	3.01	4085	1208	59.8	S,B	D
2	AIN (1-2D)	98.88	R	8.84	229.8	3.400	3.01	4086	1220	75.5	S,B	D
3	AIN (29-2A)	99.14	R	9.12	229.9	3.280	2.99	4088	1206	61.1		
4	AIN (29-2B)	99.01	R	9.12	228.8	3.280	2.99	4089	1207	56.2		
5	AIN (32-2A)	100.56	R	9.04	236.3	3.320	3.00	4090	1231	68.8		D
6	AIN (32-23)	100.56	R	9.04	236.4	3.320	3.00	4091	1207	72.6		D
7	AIN (34-2B)	103.02	R	9.22	247.1	3.260	3.01	4092	1229	70.6		
8	AIN (34-2D)	103.25	R	9.23	247.4	3.260	3.01	4093	1230	70.0		
9	AIN (1-2E)	99.16	R	8.92	230.9	3.370	3.00	4094	1221	83.0	S,B	D
10	AIN (1-2F)	99.21	R	8.92	230.9	3.360	3.00	4095	1216	68.2	S	D
11	AIN (14-2B)	101.40	R	9.35	240.4	3.210	3.00	4096	1212	61.1	S	
12	AIN (14-2F)	101.50	R	9.35	238.8	3.220	3.01	4097	1205	66.8	S	
13	AIN (18-2A)	100.51	R	9.22	236.2	3.260	3.01	4098	1211	62.7	S	
14	AIN (34-2C)	103.15	R	9.22	248.3	3.260	3.01	4099	1225	72.6	S	
15	AIN (35-2B)	103.35	R	9.22	247.7	3.260	3.01	4100	1233	89.7	S	
16	AIN (35-2C)	102.87	R	9.19	246.1	3.260	3.00	4101	1213	61.2	S	
17	AIN STD (36-2A)	102.18	R	9.12	242.5	3.290	3.00	4102	1210	73.6	S	D
18	AIN STD (36-2B)	101.60	R	9.12	242.5	3.290	3.00	4103	1231	91.5	S,B	D
19	AIN STD (36-2C)	102.11	R	9.12	243.4	3.290	3.00	4104	1226	69.0	S	D
20	AIN STD (36-2E)	102.08	R	9.12	242.7	3.290	3.00	4105	1208	77.4	S	D
21	AIN STD (36-2F)	102.13	R	9.12	243.4	3.290	3.00	4106	NR	61.3	S	D
22	AIN/SiC(90FB)	101.05	R	9.18	240.1	3.258	2.99	4131	1225	45.3		
23	AIN/SiC(100T)	101.45	R	9.18	241.6	3.265	3.00	4132	1252	68.5		
24	AIN/SiC(100B)	101.21	R	9.11	238.4	3.261	2.97	4133	1198	41.2		
25	AIN/SiC(90ST)	100.45	R	9.18	236.9	3.245	2.98	4134	1205	35.8		
26	AIN/SiC(90FT)	101.30	R	9.21	241.2	3.242	2.99	4135	1219	49.8		
27	AIN/SiC(90SB)	101.07	R	9.19	239.4	3.240	2.98	4136	1214	56.6		
28	AIN/SiC(50ST)	101.00	R	9.36	241.7	3.189	2.98	4137	1230	45.8		
29	AIN/SiC(50FB)	101.08	R	9.29	239.7	3.231	3.00	4138	1222	45.8		
30	AIN/SiC(50SB)	101.00	R	9.40	240.9	3.174	2.98	4139	1224	51.2		
31	AIN/SiC(40SB)	101.30	R	9.38	240.9	3.187	2.99	4140	1233	50.4		D

TABLE 2.1. ARO TEST MATRIX

A	B	C	D	E	F	G	H	I	J	K	L	M
Ref. No.	Tile Material Identification	Tile Dia. (mm)	Tile Shape	Tile Thck (mm)	Tile Mass (gr)	Tile Dens. (g/cm³)	A.D. (g/cm²)	Shot No.	Velocity (m/s)	Pr (mm)	Al Length	Sponsor
32	AlN/SiC(25SB)	101.42	R	9.39	242.9	3.200	3.00	4141	1226	49.3		
33	AlN/SiC(25FT)	101.39	R	9.32	241.8	3.215	3.00	4142	1223	43.9		
34	SiC(S)(G9)	101.00	R	9.44	242.7	3.156	2.98	4143	1222	44.9		
35	SiC(S)(K1)	109.20	R	9.46	271.4	3.160	2.99	4144	1227	45.4		
36	SiC(S)(K2)	109.20	R	9.47	272.6	3.170	3.00	4145	1227	45.4		
37	AlN or SiC(K3)	109.20	R	9.49	272.7	3.163	3.00	4146	1225	29.0		
38	SiC(K3)	109.20	SQ	9.49	272.7	3.163	3.00	4146	1225	30.3		
39	SiC(S)(K3)	109.20	SQ	9.49	272.7	3.163	3.00	4146	1225	29.0		
40	AlN/SiC(25ST)	101.39	R	9.33	242.2	3.221	3.01	4147	1220	44.9		
41	AlN/SiC(5SB)	101.33	R	9.33	240.8	3.211	3.00	4148	1224	47.0		
42	AlN/SiC(5ST)	101.15	R	9.31	240.3	3.214	2.99	4149	1212	43.1		
43	AlN/SiC(5FT)	100.90	R	9.59	238.3	3.119	2.99	4150	1217	53.4		
44	AlN/SiC(5FB)	100.90	R	9.65	238.9	3.095	2.99	4151	1217	41.0		
45	SiC(S)(G10)	101.00	R	9.38	240.5	3.160	2.96	4152	1208	38.6		
46	AlN/SiC(25FB)	101.42	R	9.30	241.7	3.214	2.99	4153	1218	47.7		
47	AlN or SiC(40ST)	101.43	R	9.29	241.0	3.213	2.98	4154	1225	49.9		D
48	AlN/SiC(50FT)	100.95	R	9.31	239.8	3.232	3.01	4155	1227	42.9		
49	AlN or SiC(60FT)	100.80	R	9.33	241.9	3.213	3.00	4156	1212	48.0		D
50	AlN or SiC(60FB)	100.90	R	9.46	239.9	3.165	2.99	4157	1218	54.5		D
51	AlN or SiC(60SB)	100.90	R	9.27	238.7	3.217	2.98	4158	1210	47.3		D
52	AlN or SiC(60ST)	100.79	R	9.30	239.0	3.230	3.00	4159	1204	44.2		D
53	AlN/SiC(75FB)	101.55	R	9.18	240.9	3.242	2.98	4160	1221	40.8		
54	AlN/SiC(75FT)	101.47	R	9.30	242.2	3.225	3.00	4161	1226	43.4		
55	AlN/SiC(75ST)	101.29	R	9.19	239.6	3.233	2.97	4162	1225	41.0		
56	AlN/SiC(75SB)	101.41	R	9.20	240.7	3.240	2.98	4163	1217	37.2		
57	AlN/SiC(SD411-8)	101.80	SQ	9.08	309.3	3.293	2.99	4173	1213	65.2		
58	AlN/SiC(SD411-9)	101.70	SQ	9.08	309.4	3.296	2.99	4174	1225	62.3		
59	AlN/SiC(N83-1)	103.40	R	8.97	246.8	3.277	2.94	4175	1222	71.3		
60	AlN/SiC(N83-2)	103.10	R	8.95	244.0	3.266	2.92	4176	1227	73.2		
61	AlN/SiC(C4202-3)	102.70	R	7.48	209.2	3.376	2.53	4177	1223	73.2		
62	AlN/SiC(C4202-4)	103.20	R	8.96	251.0	3.349	3.00	4178	1227	74.6		

TABLE 2.1. ARO TEST MATRIX

A	B	C	D	E	F	G	H	I	J	K	L	M
Ref. No.	Tile Material Identification	Tile Dia. (mm)	Tile Shape	Tile Thck (mm)	Tile Mass (gr)	Tile Dens. (g/cm^3)	A.D. (g/cm^2)	Shot No.	Velocity (m/s)	Pr (mm)	Al Length	Sponsor
63	AlN/SiC(SD411-6)	100.40	R	9.23	237.4	3.249	3.00	4179	1225	66.1		
64	AlN/SiC(SD411-7)	100.10	R	9.12	235.4	3.280	2.99	4180	1201	70.1		
65	TiB2-GTRI(HP69)	76.00	R	13.2	235.5	3.933	5.19	4233	1217	22.0		G
66	TiB2-GTRI(HP74)	76.10	R	13.18	237.2	3.957	5.22	4234	1223	20.0		G
67	TiB2-GTRI(HP75)	76.17	R	13.23	241.7	4.009	5.30	4235	1218	9.5		G
68	AS75SG41	101.02	R	16.00	338.5	2.640	4.22	4571	1214	7.0		D
69	AlN50	101.73	R	19.43	502.5	3.182	6.18	4572	1203	32.6		D
70	AlN48	101.22	R	16.26	422.4	3.228	5.25	4573	1225	48.3		D
71	AS75SG40	100.97	R	13.46	339.3	3.148	4.24	4574	1208	5.0		D
72	AS50F46	101.22	R	17.15	419.9	3.043	5.22	4575	1212	23.7		D
73	AS50F45	100.76	R	13.46	336.4	3.134	4.22	4576	1216	6.0		D
74	AS50F54	100.79	R	13.34	336.4	3.161	4.22	4577	1229	10.0		D
75	AS75SG43	100.71	R	16.84	425.0	3.168	5.34	4578	1216	1.0		D
76	AS75SG42	100.84	R	16.76	424.2	3.169	5.31	4579	1214	1.0		D
77	AS50F47	100.71	R	16.81	427.6	3.193	5.37	4580	1228	1.0		D
78	603PA4	109.83	R	19.18	573.4	3.156	6.05	4581	1209	5.0		D
79	603PA3	109.98	R	19.35	573.6	3.120	6.04	4582	1224	0.5		D
80	AlN49	100.66	R	16.51	423.0	3.220	5.32	4583	1220	10.0		D
81	AlN51	100.79	R	22.66	586.6	3.245	7.35	4584	1229	17.8		D
82	AlN52	101.04	R	19.43	502.5	3.225	6.27	4585	1224	33.5		D
83	AlN53	100.84	R	22.78	587.5	3.229	7.36	4586	1224	26.3		D

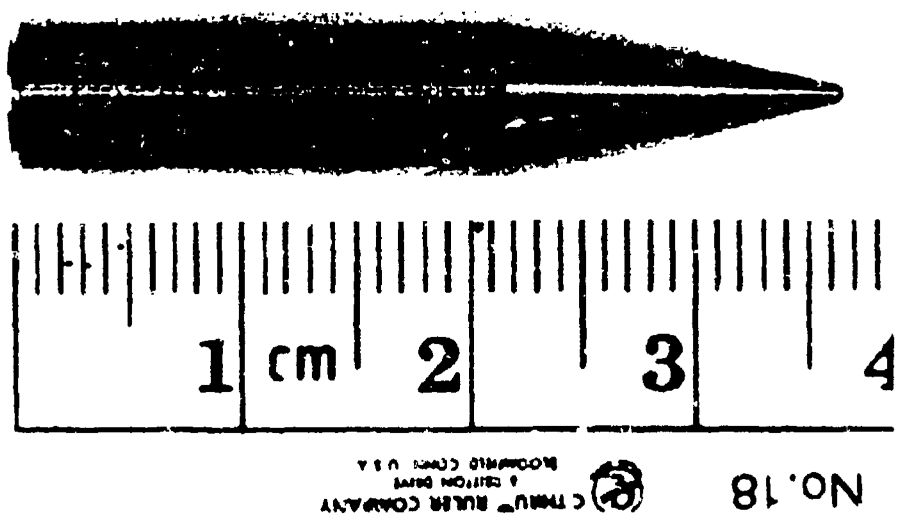

Figure 2.1. Photograph of SLAP Core.

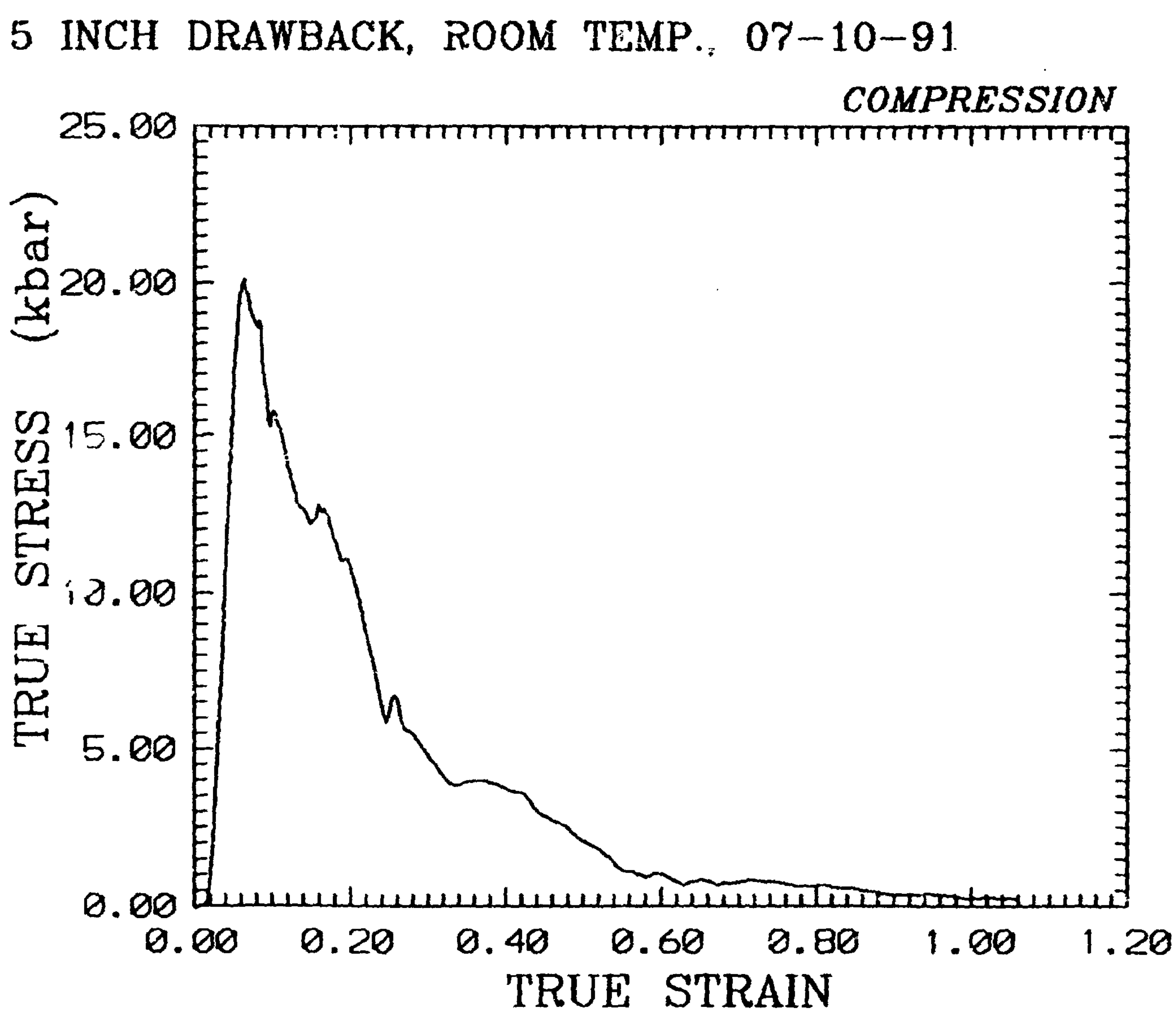

Figure 2.2. Stress-Strain Curve for SLAP Tungsten Alloy.

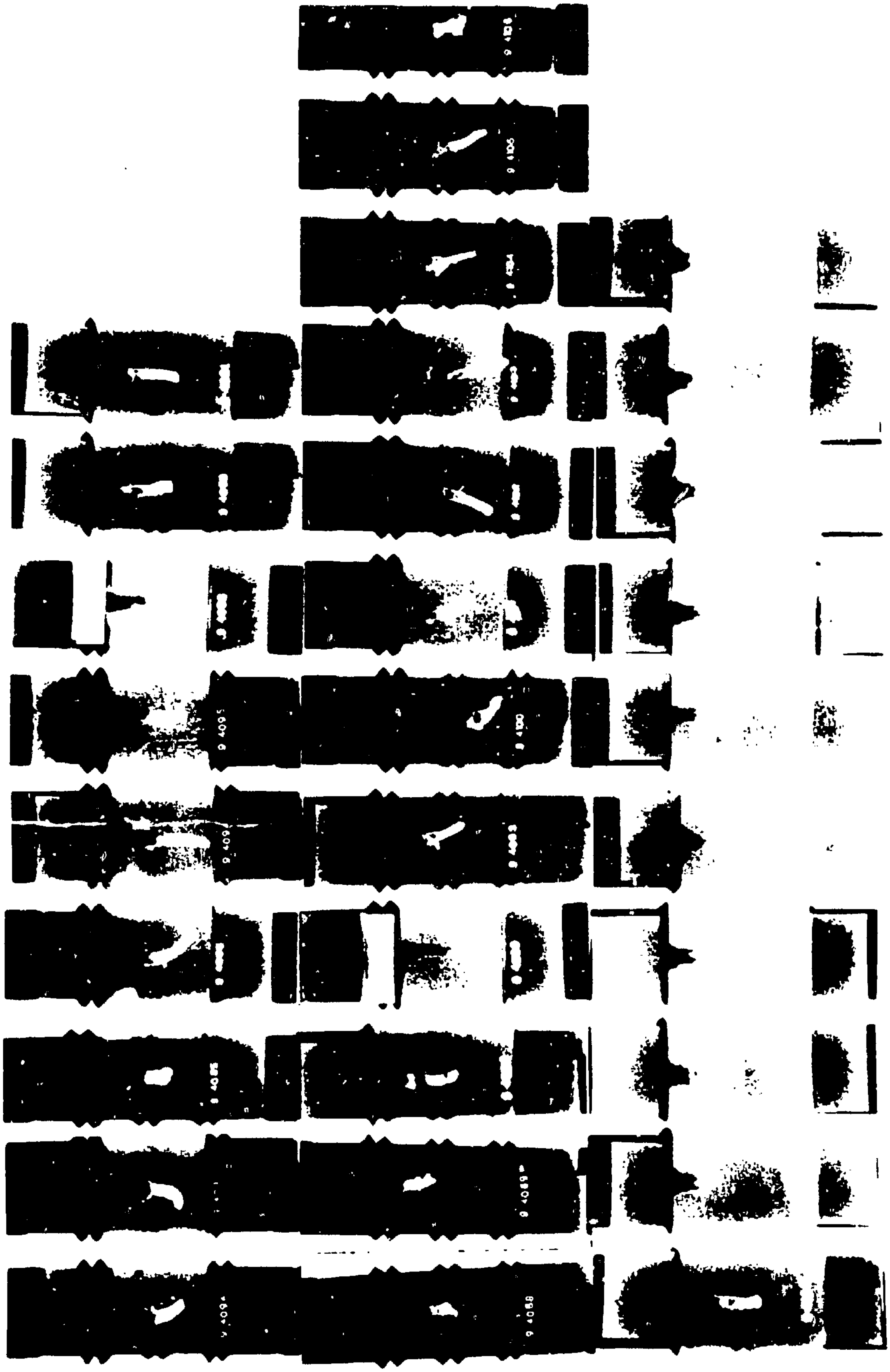

Figure 2.3. Target Radiographs.

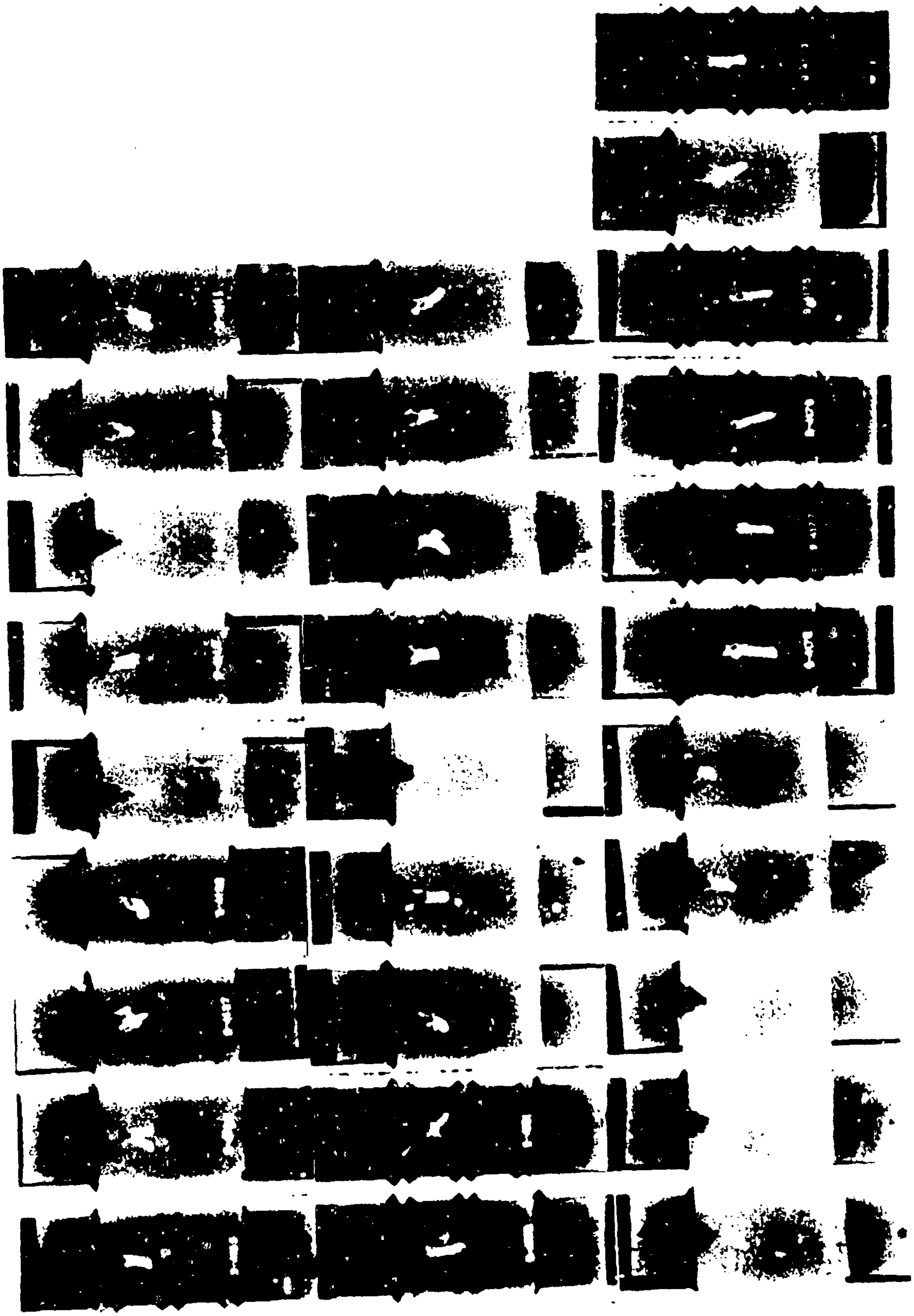

Figure 2.4. Target Radiographs.

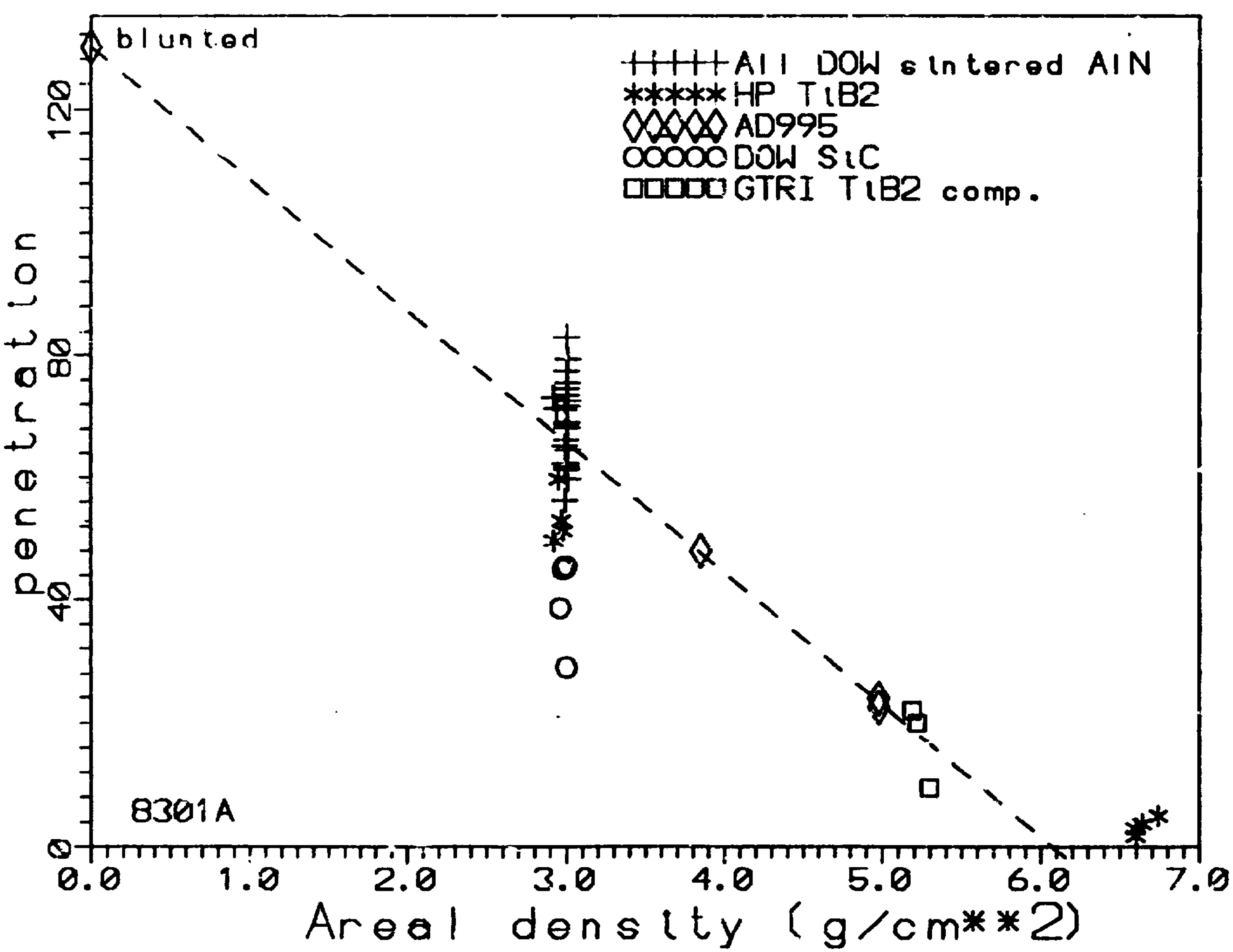

Figure 2.5. Comparative Performance of 3 g/cm² Tiles.

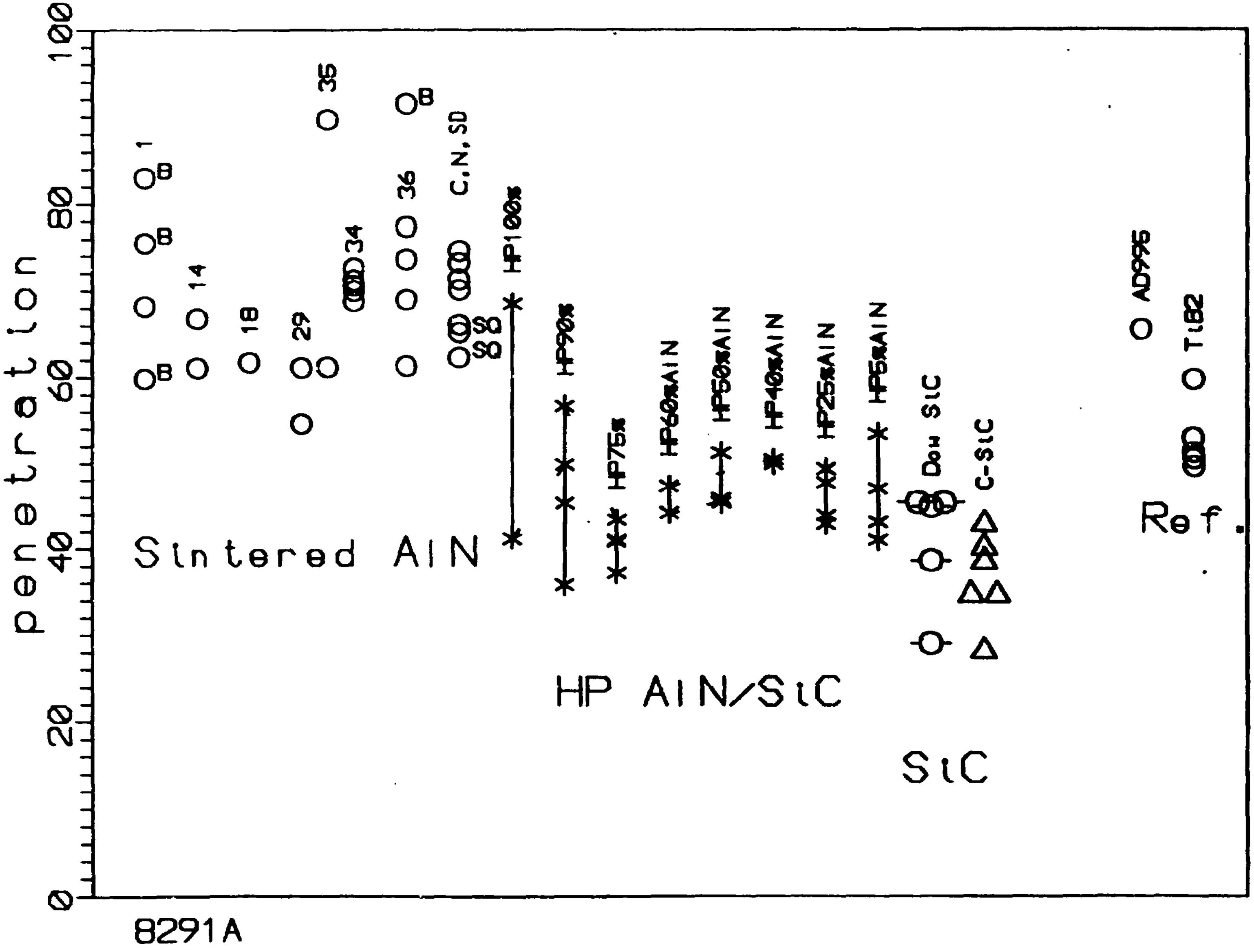

Figure 2.6. Penetration in Substrate By Ceramic Group.

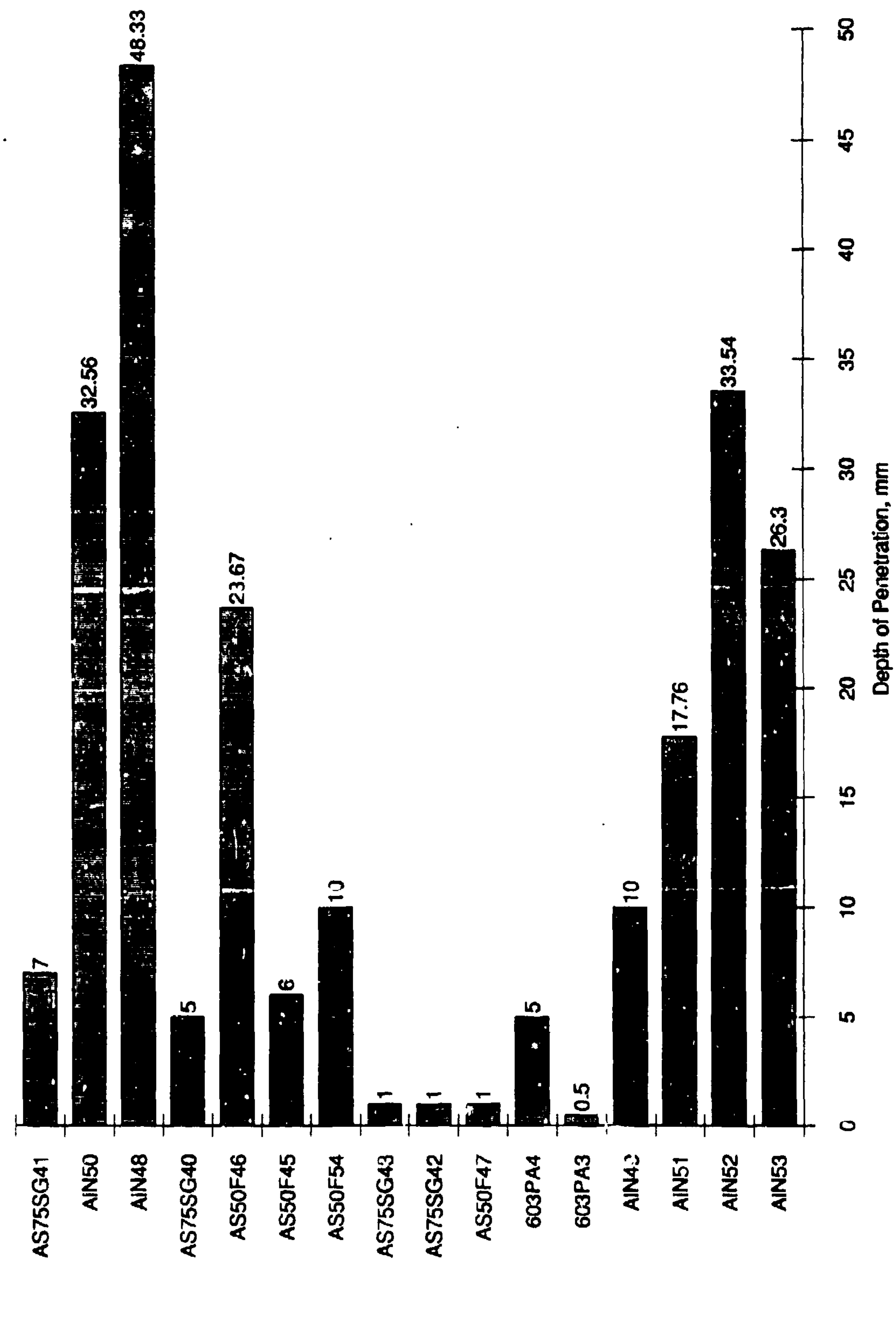

Figure 2.7. Depth of Penetration for AlN/SiC Ceramics.

SECTION 2
REFERENCES

1. J. Thompson, Combat Vehicle Survivability Symp., Gaithersberg, MD, March 1991.

2. D. Yaziv, G. Rosenberg, and Y. Partom, "Differential Ballistic Efficiency of Applique Armor," 9th Int'l. Ballistic Symp., May 1986.

3. S. Bless, Z. Rosenberg, and B. Yoon, "Hypervelocity Penetration of Ceramics," Int. J. Impact Eng. 5:165-171, 1987.

4. Z. Rosenberg, S. Bless, Y. Yeshurun, and K. Okajima, "A New Definition of Ballistic Efficiency of Brittle Materials Based on the Use of Thick Backing Plates," in Impact Loading and Dynamic Behavior of Materials, ed. C.Y. Chiem, H.D. Kunze, L.W. Meyer, DGM Informationsgesellshaft, 1988.

5. P. Woosley, S. Mariano, and D. Kokidko, "Alternative Test Methodology for Ballistic Performance Ranking of Armor Ceramics, 5th TACOM Armor Coordinating Conf., March 1989.

6. I. Mellgard, L. Holmberg, and L.G. Olsson, "An Experimental Method to Compare Ballistic Efficiency of Different Ceramics Against Long Rod Projectiles," 11th Int'l. Ballistics Symp. Brussels, May 1989.

7. C.E. Anderson and B.L. Morris, "The Ballistic Performance of Confined Al_2O_3 Tiles," submitted to *Int. J. Impact Engr.*, August 1991.

8. R. Banerjee and S.J. Bless, "Results of Compression Hopkinson Bar Testing of Olin SLAP Bullets," University of Dayton Report UDR-TM-91-21, August 1991.

9. S.J. Bless, D.L. Jurick, S.P. Timothy, and M.A. Reynolds, "Ballistic Impact Behavior of SiC Reinforced Aluminum Alloy Matrix Composites," International Conference on Shock Wave and High Strain Rate Phenomena in Materials (Explomet 90), San Diego, CA, 12-17 August 1990.

10. W. Rafaniello, Paper presented at 92nd Annual Meeting American Ceramics Society, Dallas, TX, April 1990.

SECTION 3

RESULTS OF DOP TESTING WITH L/D = 10 LONG ROD PENETRATORS

Work reported herein was sponsored by the U.S. Army Research Office (ARO) and by Dow Chemical Corporation. The Project Manager for ARO was Dr. Kalaisam Iyer. The Project Manager for Dow was Dr. William Rafaniello. Experiments were conducted in the facilities of the University of Dayton Research Institute Impact Physics Laboratory. This report constitutes a final topical report.

Hot pressed TiB_2/Al_2O_3 samples were provided by Georgia Tech Research Institute (GTRI). Kathryn Logan was the Project Manager for GTRI. Range technicians Stephen Hanchak and Thomas Williams are commended for their support in assembling target, conducting ballistic tests, and preparing targets for analysis.

1. EXPERIMENT DESIGN

Depth-of-penetration (DOP) experiments were conducted to identify the best performing ceramic against quarter scale Long Rod Penetrators (LRP). This test procedure has become popular in recent years as a tool for designing armor elements[1-4].

Testing was conducted with quarter scale, 65 g tungsten L/D=10 rods supplied by Mr. Bill Gooch at Ballistic Research Laboratory (BRL). The rods had a hemispherical nose. The rod diameter was 7.82 mm and the length was 78.74 mm. The rods were launched on the University of Dayton Research Institute (UDRI) 30 mm smooth bore Range 1.

The targets were embedded in RC27 certified 4340 steel. We checked the hardness on one target section after the shot and measured Brinnell 275 which converts to HRC29. This material is a surrogate for RHA, although the hardness was on the low side of the range for MIL-SPEC-12560.

The steel rounds were 6-inches diameter manufactured by Copperweld Steel. The steel rounds were machined with round cavities to accept ceramic tiles supplied for testing. The cavities were individually machined to match individual tiles which allowed a "slip fit" of the tile into the steel. The tiles were cemented into the steel with Belzona A - Metal ceramic filled epoxy. A press was used to squeeze out the excess epoxy. Bond lines under the tile, examined post shot, were typically 0.25 mm thick.

2. RESULTS OF EXPERIMENTS

The physical properties of each ceramic tested and the results of the testing are given in Table 3.1. Columns in this table are identified as follows:

A: Tile material

B: Tile diameter (mm)

C: Tile thickness (mm)

D: Tile mass (g)

E: Tile density (g/cm^3)

F: Tile areal density (g/cm^2)

G: Shot number (Range 1)

H: Impact velocity (m/s)

I: Penetration in steel below tile (mm)

J: Remarks (Y is yaw, MR is mass of recovered projectile, and DR is diameter of recovered projectile)

Figure 3.1 is a comparison of our data for 4340 steel compared to Southwest Research Institute (SWRI) data for the nominally the same steel. The SWRI rod was a 75 g tungsten rod, L/D = 10, with a length of 81.8 mm. The SWRI data was contained in an unpublished report provided by Dow Chemical, USA. However, the data also appears in recent publications by Charles Anderson (SWRI) on penetration into steel and into alumina.

We found that our data agreed very well with the SWRI data at 1500 m/s. However, both their data point at 1500 and our points lie significantly above the trend of their data. This may be because four out of their seven shots above 1200 m/s had significant yaw.

Nevertheless, for purpose of establishing a reference penetration, we have fit a straight line to the L/D = 10 SWRI data and our two points. The fit is shown in Figure 3.2. The equation of the best fit line is:

$$P/L = .00108V - 0.73$$

We have used this equation to establish reference penetration data.

Data are presented in the format of plots of W_R versus W_C. W_C is defined as the areal density of the ceramic. W_R is the areal density penetrated in the substrate (density x penetration, P_R). W_{REF} is the areal density penetrated in the substrate if no tile is present. The differential mass efficiency, Δe_m, of the ceramic relative to the substrate is the slope of the line on the (W_R, W_C) plot. It can also be computed from

$$\Delta e_m = \frac{W_{REF} - W_R}{W_C}$$

Figure 3.3 compares the areal density of steel penetrated below the ceramic (W_R) with the areal density of the ceramic (W_C) for our AD90 data with the SWRI data. We find slightly higher penetration for the thicker tiles (W_C = 15 g/cm²). However, this effect diminishes if one takes into account the difference in velocity in the SWRI shots as shown later in Figure 3.5. Using equation (1), we have the AD90 results shown for our data (triangles) and SWRI data (circles); we calculated e_m of about 1.5, whereas SWRI data gives an e_m of about 1.8.

If we use our measured value of reference penetration at 1500 m/s to compute our e_m, we get 1.7 as our e_m value. If we use the SWRI reference curve we also get an e_m = 1.7 as their average e_m value for AD90 at 15 g/cm². Thus, there may be no disparity between our data, only an apparent offset caused by using equation (1). It would probably be prudent to reanalyze the performances using a best fit to the unyawed SWRI data as reference for their shots and our measured referance penetration as a reference for our shots.

Figure 3.4 shows the penetration data from Table 3.1 for the AD90, hot-pressed AlN, and sintered AlN specimens at 15 g/cm². The scatter in these data is relatively small. Likewise, the Material 34 data points at W_C = 15 g/cm² fall rather close together. Table 3.2 provides SWRI penetration data for Dow supplied materials. Note that the SWRI data for Material A at 15 g/cm² is very suspect for two reasons: (1) the yaw in one shot (#66) was 5.6 degrees, and (2) the datum is very much less than our two shots on Materials A and C. Figure 3.5 displays the SWRI DOP data for ceramics of 15 g/cm² areal density.

Figure 3.6 displays the penetration data for hot-pressed AlN, sintered AlN, and TiB_2/SiC at 10 g/cm². The scatter in these data is relatively small. Materials 28 and 34 are the same, and the penetrations fall very close together. Material 29 and TiB_2/SiC showed appreciable data scatter at 10 g/cm². Figure 3.7 shows the SWRI DOP data for ceramics of areal density = 10 g/cm².

3. CONCLUSIONS

Tables 3.2 and 3.3 present the areal densities of the ceramics, W_C, penetrated steel substrate (W_r), and calculated ballistic differential mass efficiency, Δe_m, values for each material tested by SWRI and UDRI respectively. We used our reference penetration for steel of 76.7 mm which gives W_{REF} = 59.9 g/cm² to calculate the Δe_m values. Figures 3.9 and 3.11 show the relative Δe_m values, using equation (1) for reference data. Figures 3.8 through 3.11 present the ballistic mass efficiencies from Tables 3.2 and 3.3.

From Figures 3.8 through 3.11 it can be seen that:

(1) AlN data for UDRI and SWRI agree quite well except for some anomalies.

(2) AlN out performs AD90.

(3) The sintered AlN materials perform as well as or better than the hot-pressed AlN.

(4) TiB_2/Al_2O_3, GTRI material offered promise but was inconsistent. One sample (shot 922-1) performed exceptionally well and should be pursued further.

(5) One sample of sintered AlN (AS75S80/AM) displayed exceptional performance and should be pursued further.

TABLE 3.1. SUMMARY OF ARO PENETRATION DATA

Tile Identification	Proj.	Conf. Well	Tile Dia.(mm)	Tile Thick (mm)	Tile Mass-gr	Tile Density	A.D. g/cm²	Shot No.	V (m/s)	Pr (mm)	Remarks Y=Yaw MR=Res. Mass, DR=Dia.
4340RC27(Ref.)	.25LRP	N/A						1-204	1542	76.70	Y=0.3
4340RC27	.25LRP	N/A						1-205	1529	77.70	Y=4.1
TiB2/SiC-GTRI 769-2	.25LRP	Y	101.60	24.20	764.7	3.90	9.43	1-228	1534	50.80	Y=1.0,MR=9.55
TiB2/SiC-GTRI 921-1	.25LRP	Y	101.60	24.30	780.4	3.96	9.63	1-224	1515	41.50	Y=3.0,MR=10.47
TiB2/SiC-GTRI 764	.25LRP	Y	101.60	24.20	783.5	3.99	9.66	1-222	1537	47.70	Y=2.1,MR=10.55
TiB2/SiC-GTRI 926-1	.25LRP	Y	101.60	24.30	787.6	4.00	9.72	1-226	1528	40.10	Y=2.9,MR=9.77
AS75SG85PM	.25LRP	Y	101.57	31.12	792.0	3.14	9.77	1-266	1558	17.12	Y=0.9, MR=5.14
AIN (35-A)	.25LRP	Y	102.44	30.99	818.3	3.21	9.95	1-209	1529	46.50	Y=1.1
AIN (34-E)	.25LRP	Y	102.10	30.54	813.3	3.25	9.95	1-217	1539	43.00	Y=2.16,MR=11.1
AS75S802AM	.25LRP	Y	100.75	31.04	794.8	3.21	9.96	1-265	1546	15.39	Y=0.5, MR=5.21
AS50F801PM	.25LRP	Y	100.92	31.06	797.0	3.21	9.97	1-269	1546	36.20	Y=1.8, MR=9.13
AS50F818PM	.25LRP	Y	100.75	31.04	795.8	3.21	9.97	1-263	1542	42.82	Y=2.0,MR=11.26
AIN (29-A)	.25LRP	Y	99.90	30.73	780.4	3.25	9.99	1-211	1524	47.27	Y=2.8,MR=25.7
AIN (28-B)	.25LRP	Y	104.39	31.12	848.5	3.21	9.99	1-208	1541	40.89	Y=0.4,MR=18.7,DR=12.0
AIN (29-B)	.25LRP	Y	99.85	30.76	775.1	3.25	10.00	1-213	1529	40.00	Y=0.6,MR=20.6
AIN (27-H)	.25LRP	Y	103.95	31.30	843.6	3.23	10.11	1-271	1535	42.04	Y=1.1, MR=10.01
TiB2/SiC-GTRI 769-1	.25LRP	Y	101.60	36.30	1162.5	3.95	14.34	1-229	1541	24.10	Y=1.9,MR=8.72
TiB2/SiC-GTRI 922-1	.25LRP	Y	101.60	36.40	1163.8	3.94	14.35	1-225	1532	1.90	Y=1.0,MR=2.9
TiB2/SiC-GTRI 925-1	.25LRP	Y	101.60	36.40	1170.2	3.97	14.43	1-227	1529	25.30	Y=0.6,MR=7.74
TiB2/SiC-GTRI 731-2	.25LRP	Y	101.60	36.30	1204.0	4.09	14.85	1-223	1537	29.60	Y=2.5,MR=8.32
AIN (35-E)	.25LRP	Y	101.22	47.83	1194.2	3.11	14.88	1-272	1555	29.59	Y=1.1, MR=7.91
AS50F31PM	.25LRP	Y	101.05	46.51	1195.4	3.20	14.89	1-267	1552	25.43	Y=1.5, MR=8.71
AIN AS50F30PM	.25LRP	Y	101.25	46.58	1202.3	3.20	14.92	1-264	1551	26.72	Y=1.2,MR=5.86
AIN (34-A)	.25LRP	Y	102.03	46.16	1221.1	3.24	14.93	1-212	1530	33.84	Y=2.9, MR=8.2
AIN (34-C)	.25LRP	Y	101.32	45.92	1205.4	3.26	14.95	1-218	1541	32.00	Y=3.0,MR=10.6, DR=11
AS75S801AM	.25LRP	Y	100.61	46.51	1190.0	3.22	14.97	1-270	1533	0.10	Y=0.2, MR=4.56
AIN (31-C)	.25LRP	Y	100.86	45.72	1198.1	3.28	15.00	1-215	1529	26.28	Y=0.8, MR=12.9
AIN (32-F)	.25LRP	Y	100.84	45.06	1198.3	3.33	15.00	1-214	1544	36.50	Y=5.3
AS75SG31AM	.25LRP	Y	100.66	46.48	1195.5	3.23	15.01	1-268	1571	22.38	Y=1.0, MR=6.81
AIN HP (A)	.25LRP	Y	100.51	46.33	1188.5	3.24	15.01	1-210	1534	28.67	Y=3.1,MR=7.1,DR=9
AIN HP (C)	.25LRP	Y	100.84	46.23	1192.5	3.25	15.02	1-216	1525	29.50	Y=1.3,MR=9,DR=11
AD90	.25LRP	Y	101.80	41.90	1224.0	3.59	15.03	1-207	1540	43.70	Y=0.7
AD90	.25LRP	Y	101.90	41.90	1228.0	3.59	15.06	1-206	1532	44.00	Y=1.3
AIN (35-F)	.25LRP	Y	101.80	47.50	1213.1	3.22	15.13	1-262	1505	27.28	Y=1.0,MR=6.61

TABLE 3.2. SWRI PENETRATION DATA AND CALCULATED BALLISTIC EFFICIENCIES

Tile Material ID	Wc g/cm²	Pr (mm)	Wr g/cm²	Δe_m
A1211	9.90	39.40	30.77	2.94
A1212	9.88	42.60	33.27	2.70
B1213	9.85	36.10	28.19	3.22
B1214	9.96	41.10	32.10	2.79
C1215	9.94	39.10	30.54	2.95
C1216	9.88	39.30	30.69	2.96
D1219	9.85	36.70	28.66	3.17
D1220	9.87	41.80	32.65	2.76
E1217	9.93	37.90	29.60	3.05
E1218	9.93	29.10	22.73	3.74
A1801	14.98	12.00	9.37	3.37
A1802	14.97	29.70	23.20	2.45
B1803	14.80	35.50	27.73	2.17
B1804	14.93	42.40	33.11	1.79
C1805	14.98	43.30	33.82	1.74
C1806	15.00	41.90	32.72	1.81
D1809	15.12	41.30	32.26	1.83
E1807	15.07	33.70	26.32	2.23
E1808	15.09	31.00	24.21	2.37

TABLE 3.3. CALCULATED BALLISTIC EFFICIENCIES

Tile Material ID	Wc g/cm^2	Pr (mm)	Wr g/cm^2	Δe_m
4340RC27(Ref.)		76.70	59.90	1.00
4340RC27		77.70	60.68	
TiB2/SiC-GTRI 769-2	9.43	50.80	39.67	2.15
TiB2/SiC-GTRI 921-1	9.63	41.50	32.41	2.85
TiB2/SiC-GTRI 764	9.66	47.70	37.25	2.34
TiB2/SiC-GTRI 926-1	9.72	40.10	31.32	2.94
AS75SG85PM	9.77	17.12	13.37	4.76
AlN (35-A)	9.95	46.50	36.32	2.37
AlN (34-E)	9.95	43.00	33.58	2.65
AS75S802AM	9.96	15.39	12.02	4.81
AS50F801PM	9.97	36.20	28.27	3.17
AS50F818PM	9.97	42.82	33.45	2.65
AlN (29-A)	9.99	47.27	36.92	2.30
AlN (28-B)	9.99	40.89	31.93	2.80
AlN (29-B)	10.00	40.00	31.24	2.87
AlN (27-H)	10.11	42.04	32.83	2.68
TiB2/SiC-GTRI 769-1	14.34	24.10	18.82	2.86
TiB2/SiC-GTRI 922-1	14.35	1.90	1.48	4.07
TiB2/SiC-GTRI 925-1	14.43	25.30	19.76	2.78
TiB2/SiC-GTRI 731-2	14.85	29.60	23.12	2.48
AlN (35-E)	14.88	29.59	23.11	2.47
AS50F31PM	14.89	25.43	19.86	2.69
AlN AS50F30PM	14.92	26.72	20.87	2.62
AlN (34-A)	14.93	33.84	26.43	2.24
AlN (34-C)	14.95	32.00	24.99	2.34
AS75S801AM	14.37	0.10	0.08	4.00
AlN (31-C)	15.00	26.28	20.52	2.63
AlN (32-F)	15.00	36.50	28.51	2.09
AS75SG31AM	15.01	22.38	17.48	2.83
AlN HP (A)	15.01	28.67	22.39	2.50
AlN HP (C)	15.02	29.50	23.04	2.45
AD90	15.03	43.70	34.13	1.71
AD90	15.06	44.00	34.36	1.70
AlN (35-F)	15.13	27.2[illegible]	21.31	2.55

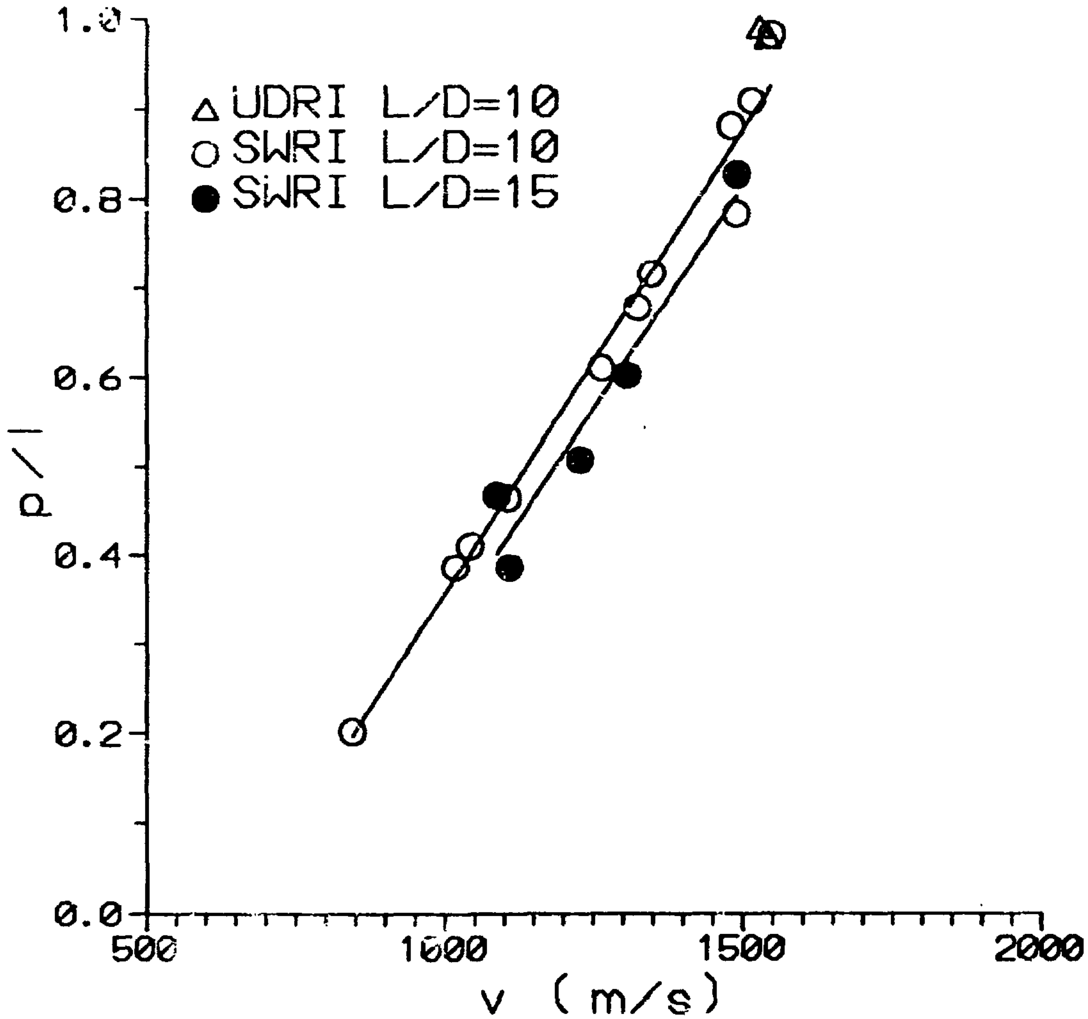

Figure 3.1. Penetration into Steel Normalized by the Length of Penetrator, L. as a Function of Strike Velocity. D is the Diameter of the Penetrator.

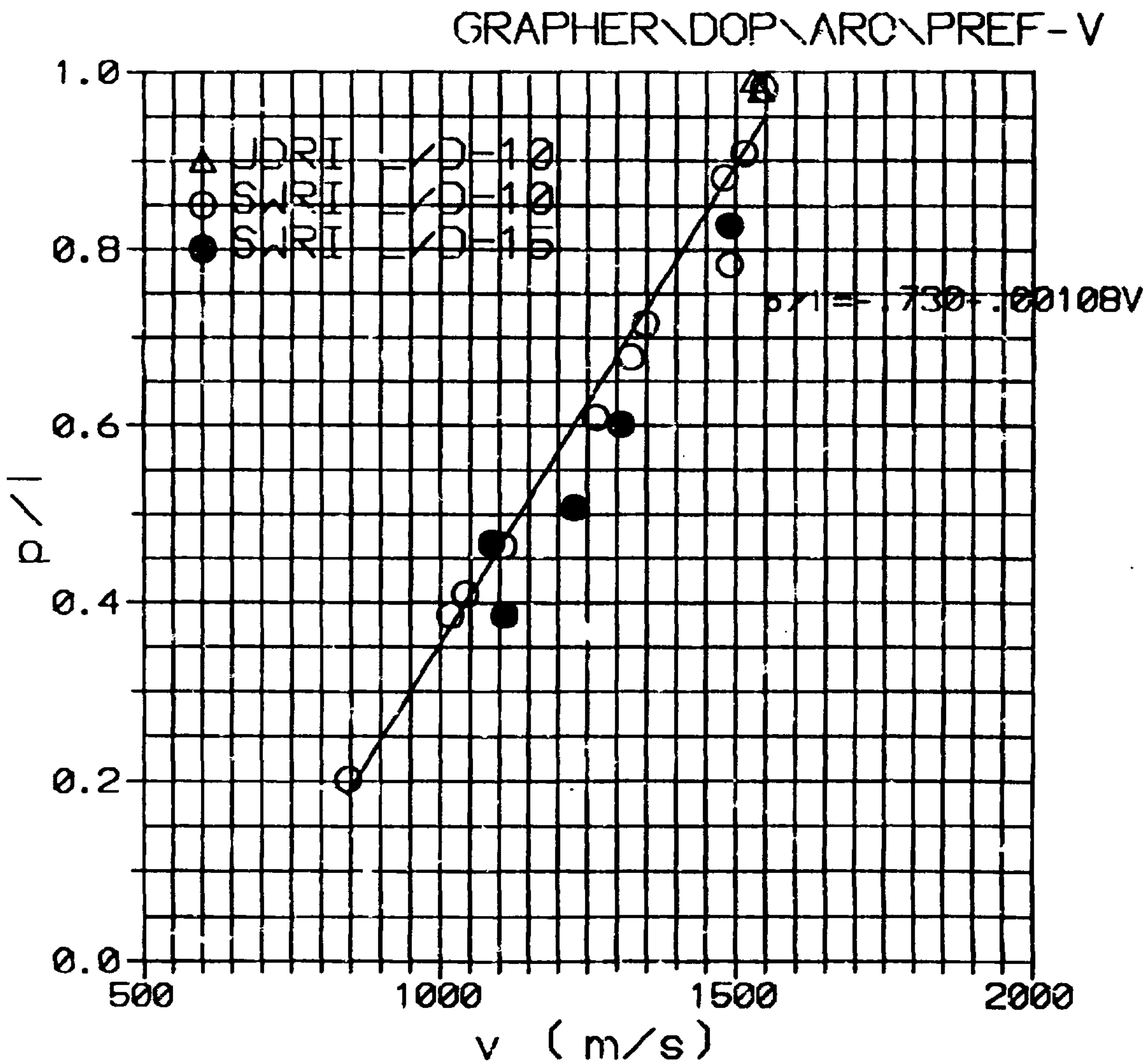

Figure 3.2. The Data Shown in Figure 3.1 with at Least Square Linear Fit to L/D = 10 Data Only.

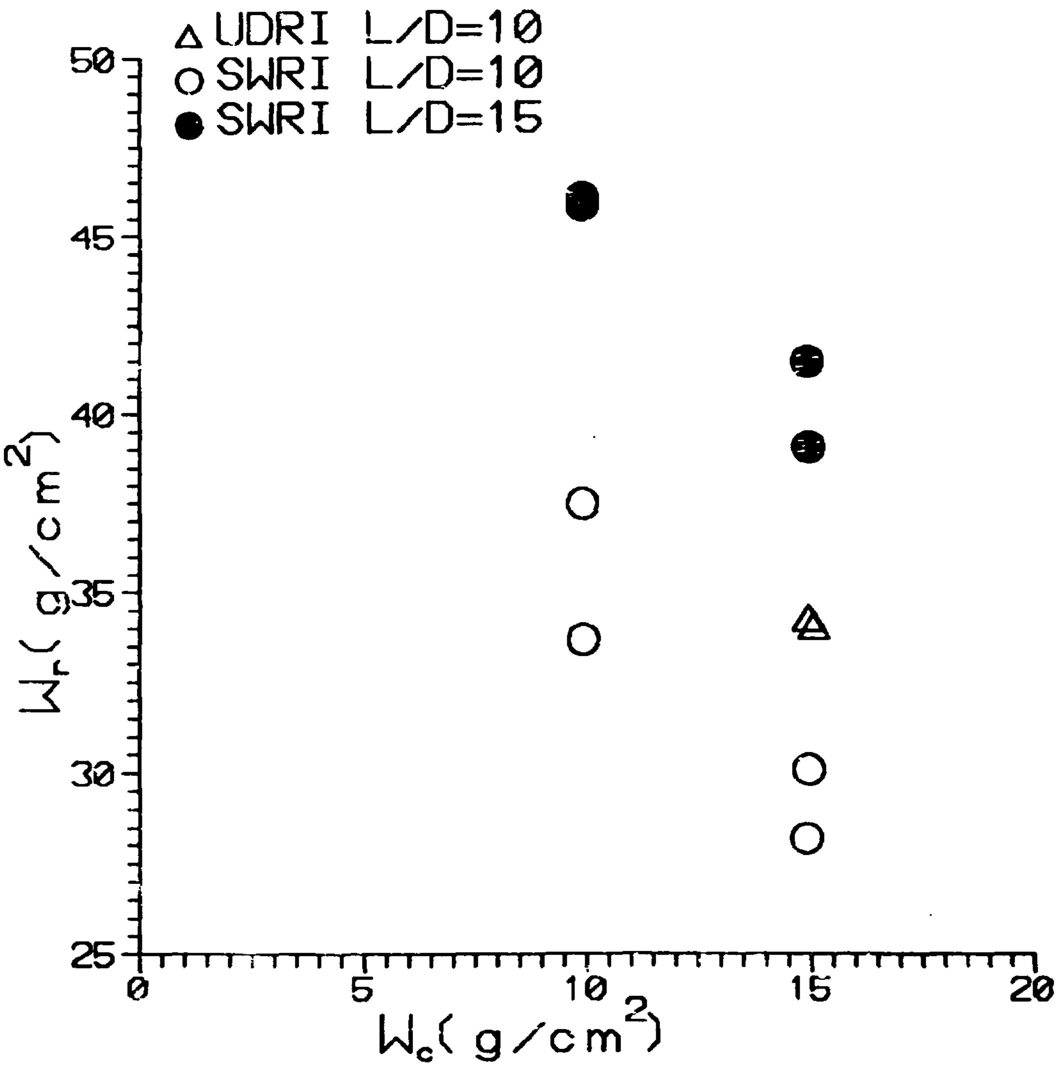

Figure 3.3. Areal Density of Steel (W_r) Penetrated Below AD90 Ceramic as a Function of the Areal Density of Ceramic (W_c).

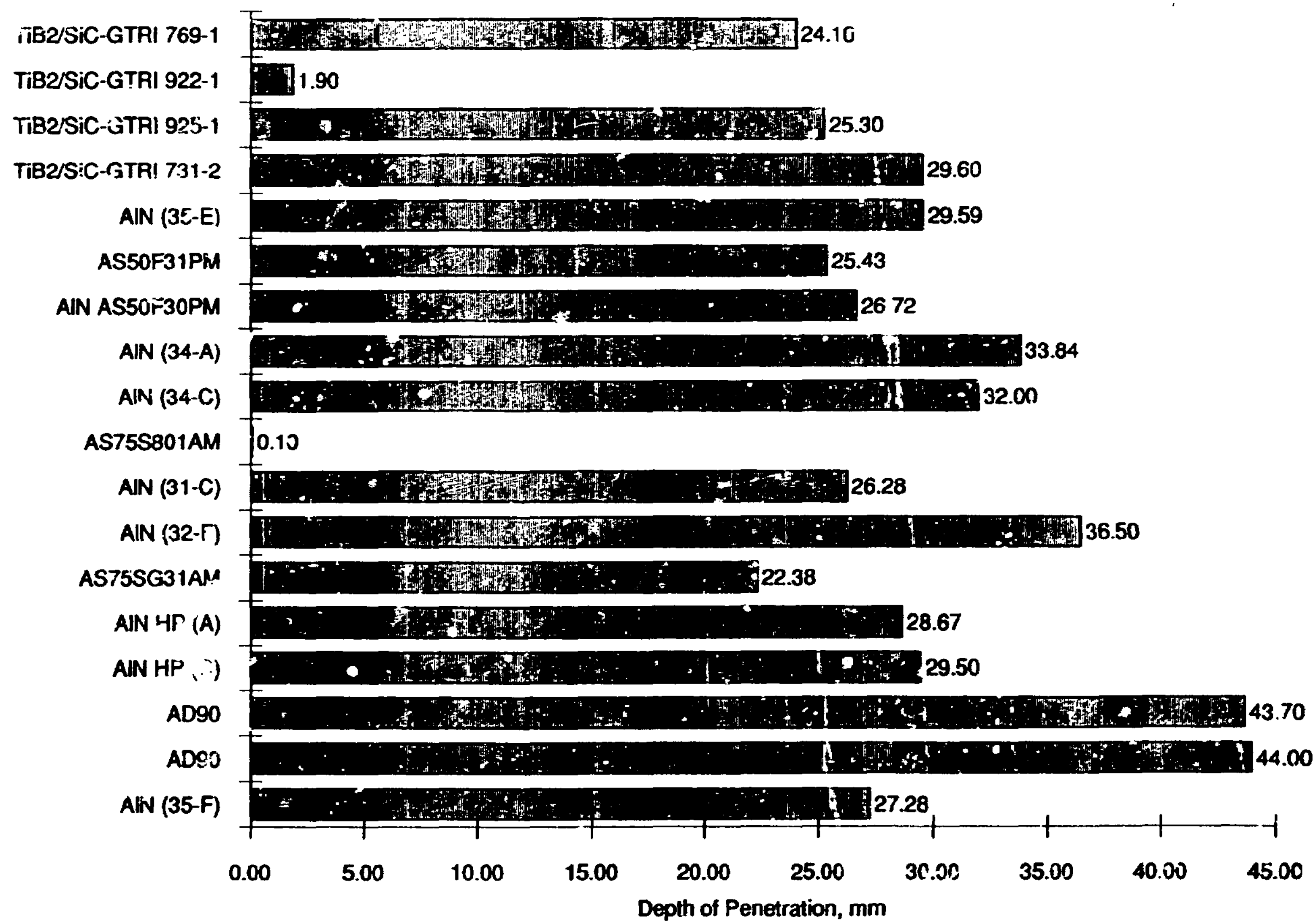

Figure 3.4. Depth of Penetration for Areal Density = 15 g/cm² Ceramics.

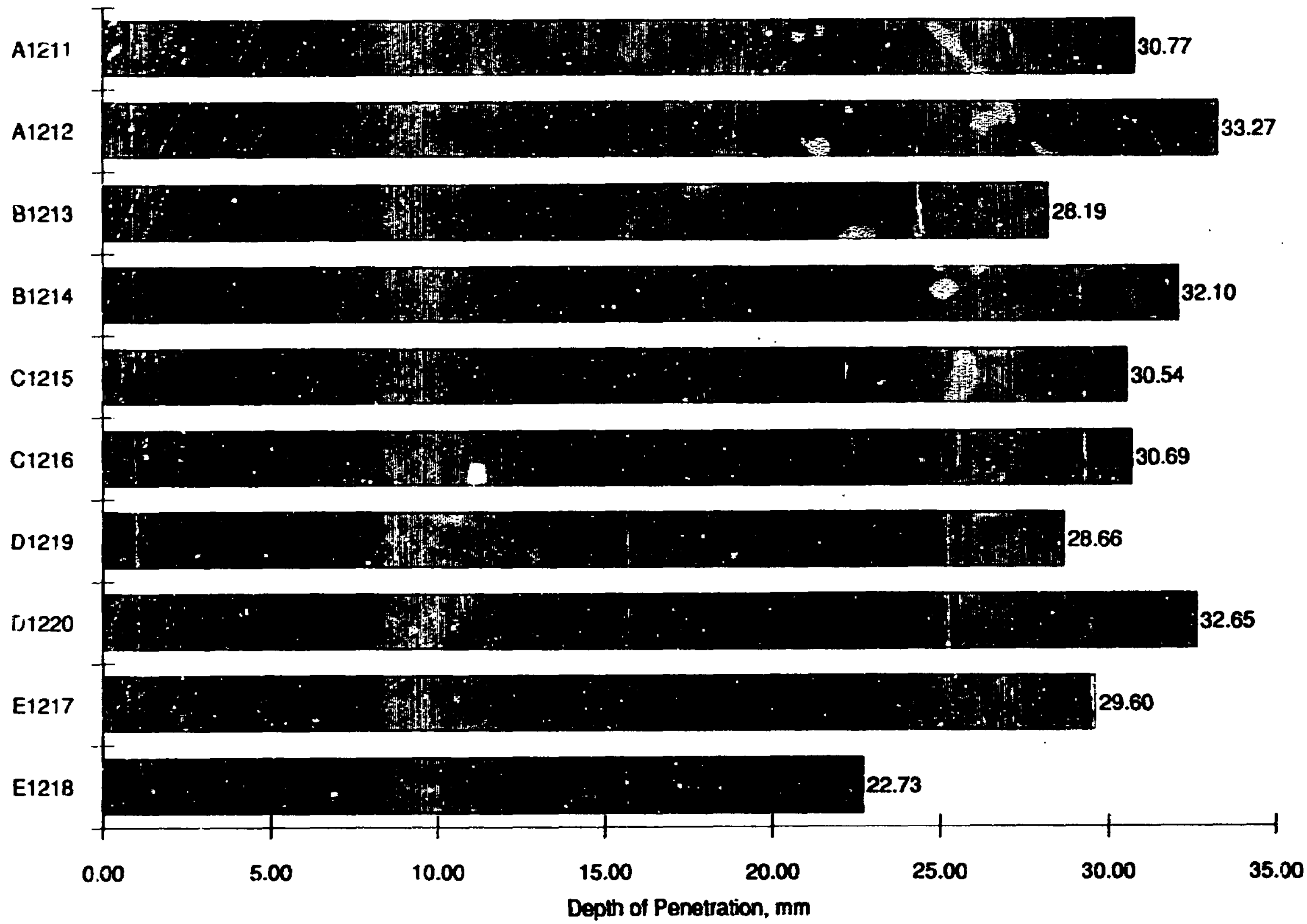

Figure 3.5. Depth of Penetration for SWRI Data at 15 g/cm² Areal Density.

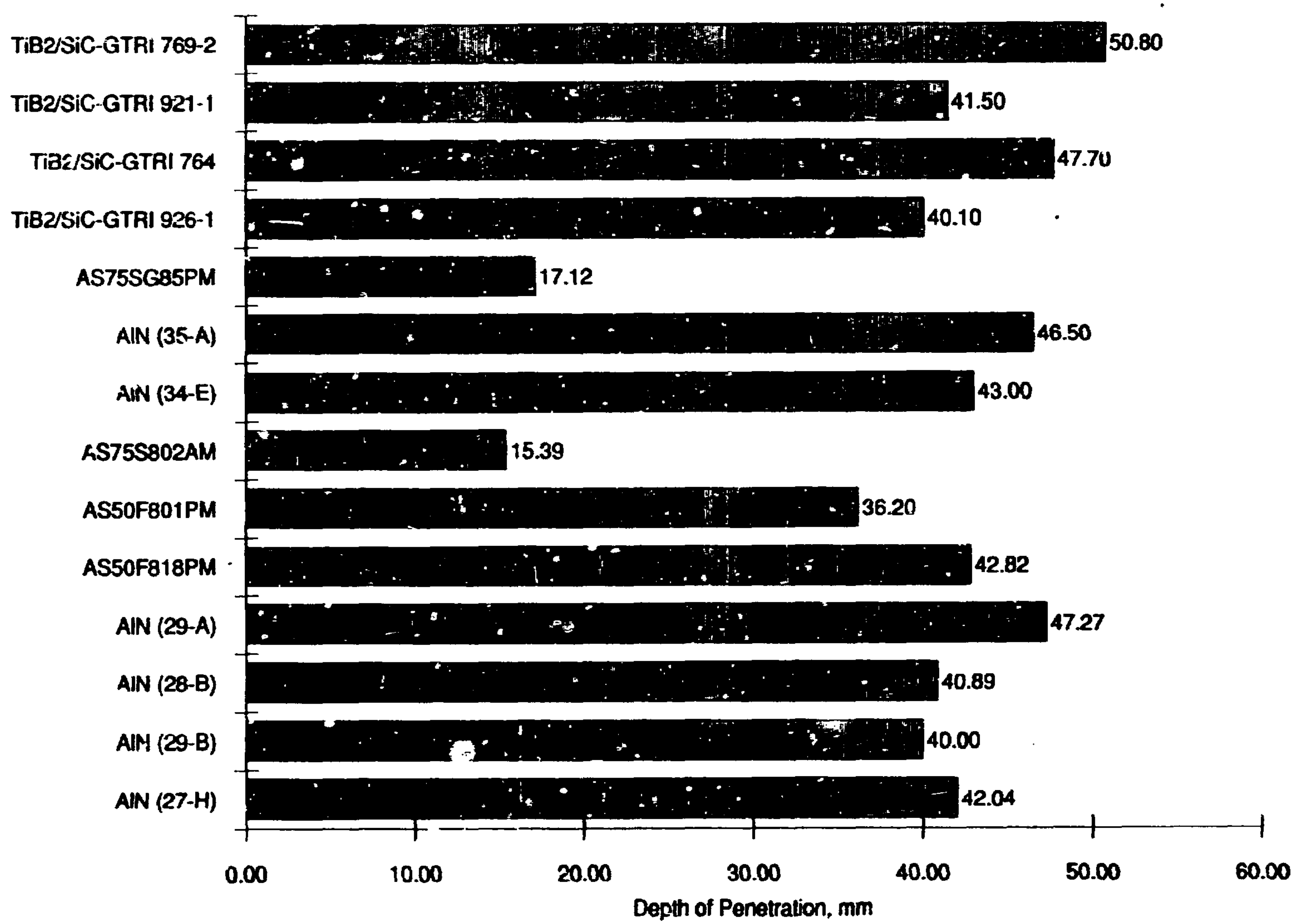

Figure 3.6. Depth of Penetration for Areal Density = 10 g/cm² Ceramics.

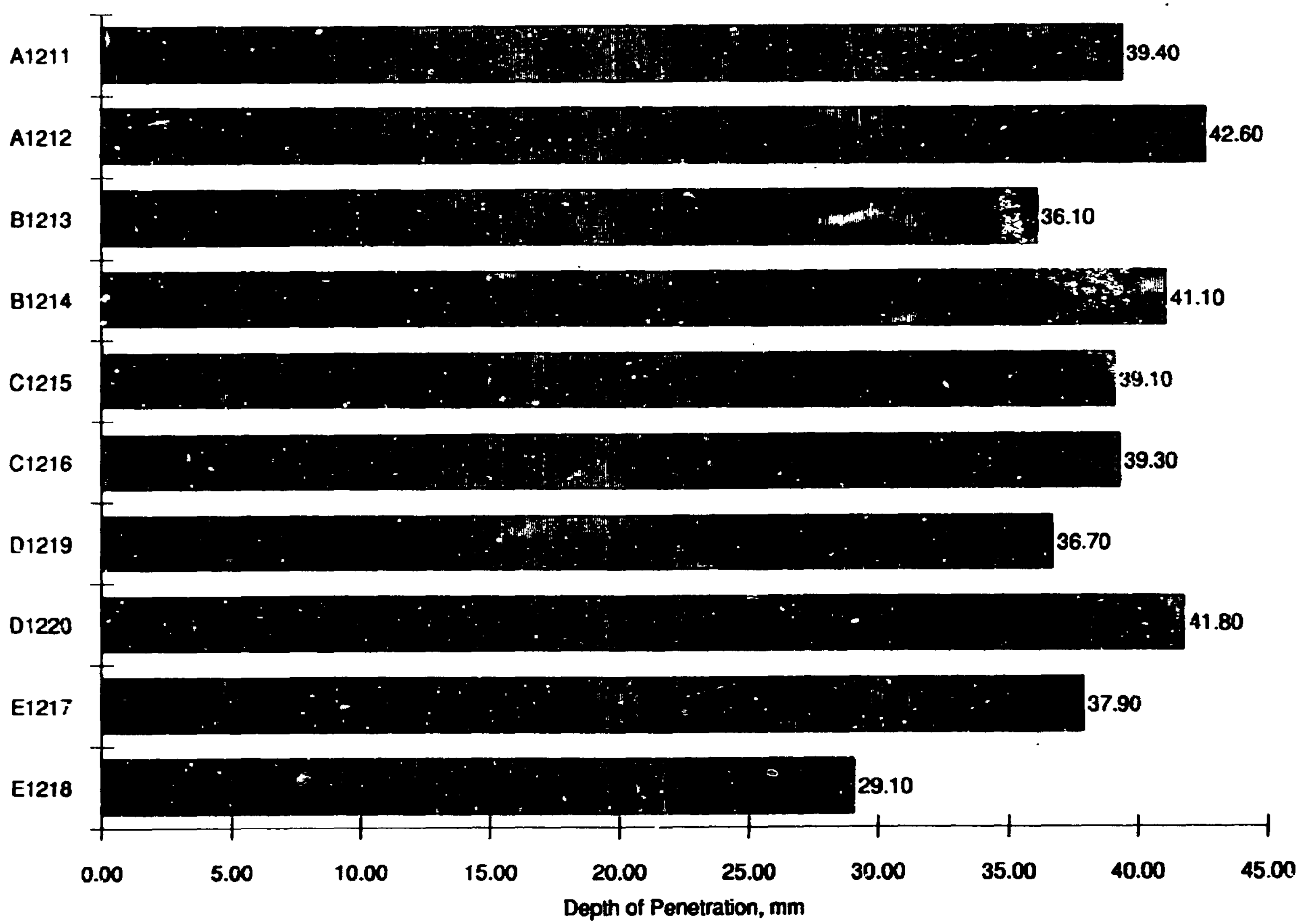

Figure 3.7. Depth of Penetration for SWRI Data at 10 g/cm² Areal Density.

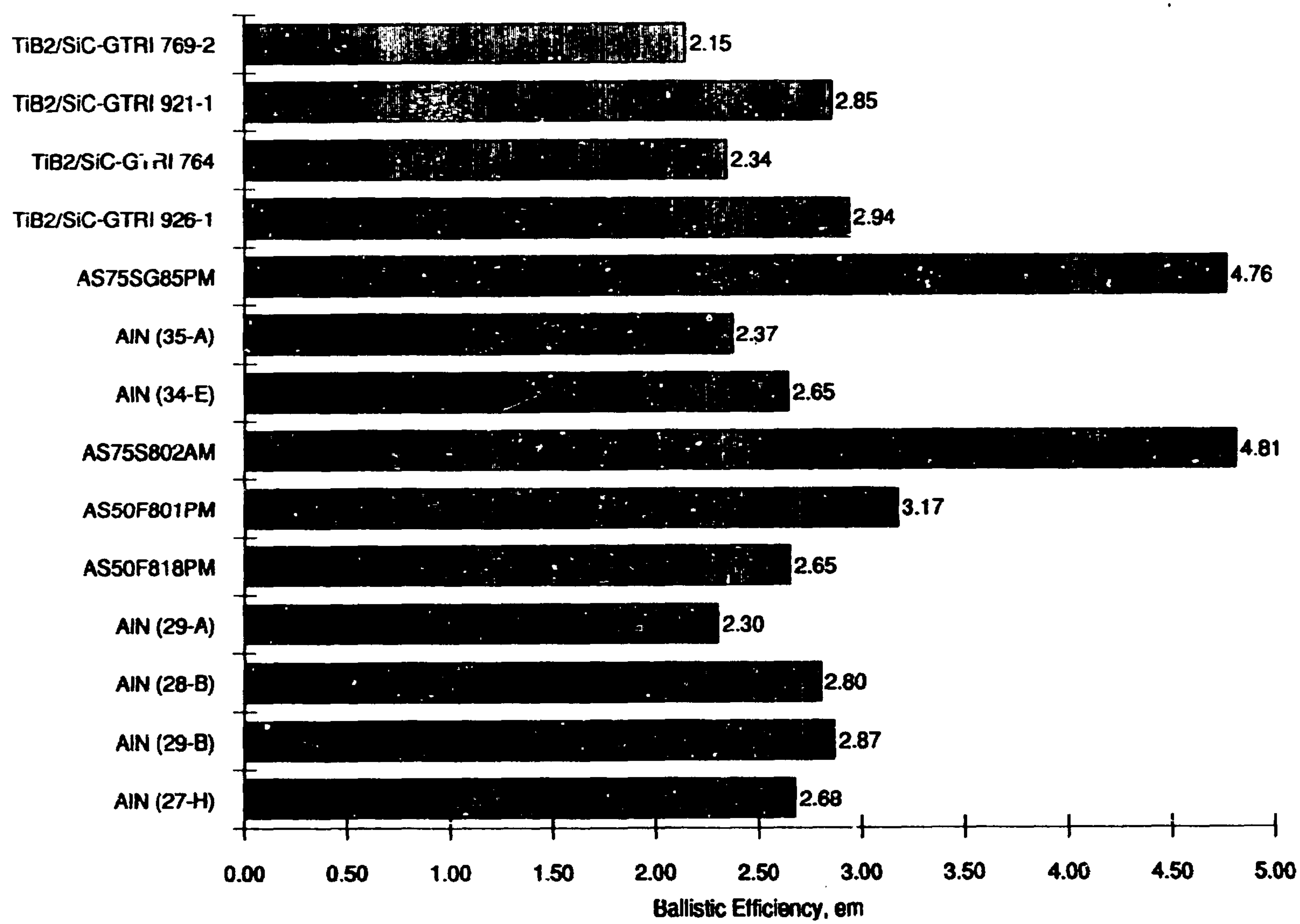

Figure 3.8. Ballistic Efficiency of 10 g/cm² Areal Density Ceramics.

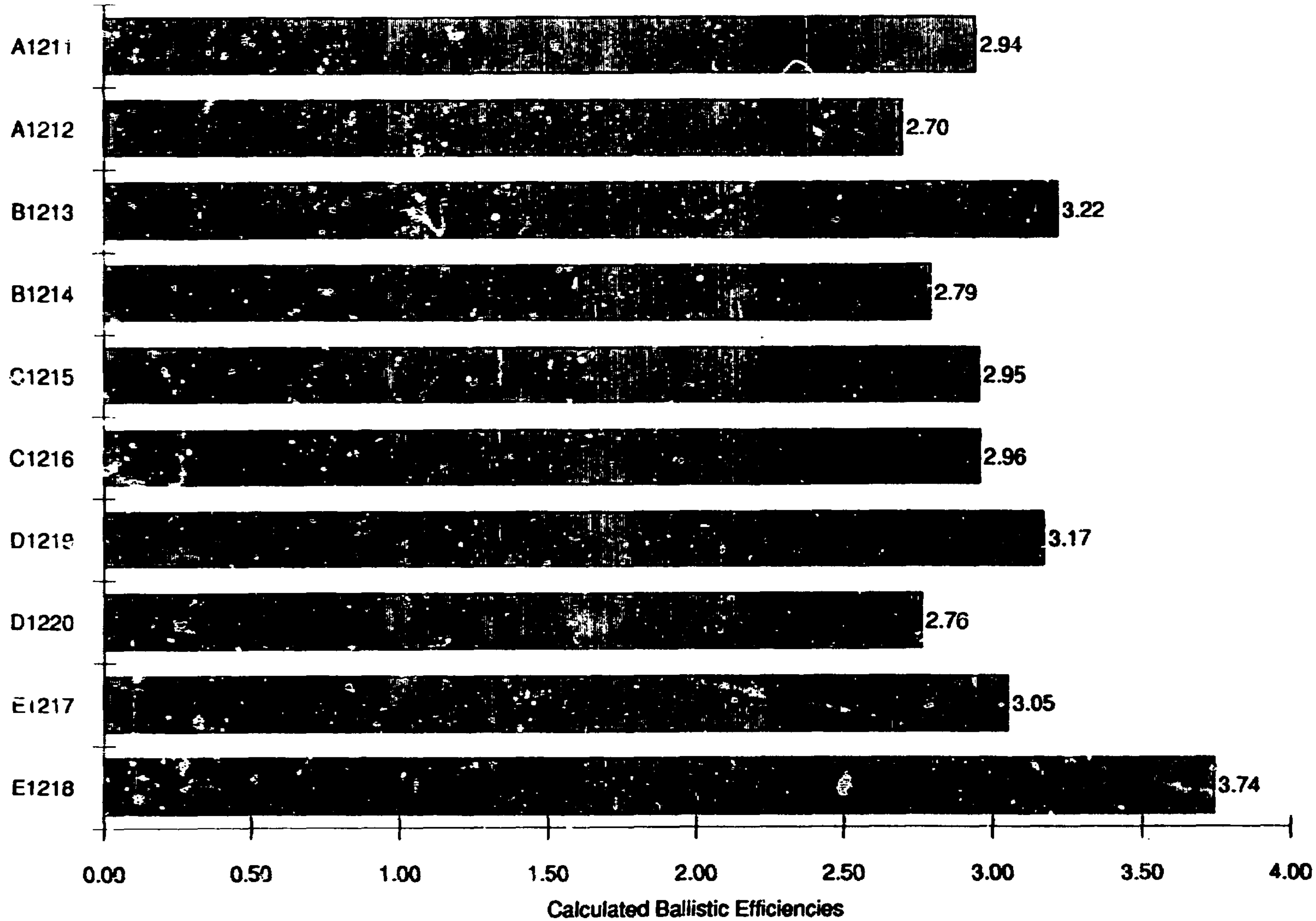

Fig. 29 SWRI Calculated Ballistic Efficiencies for Areal Density = 10 g/cm² Ceramics.

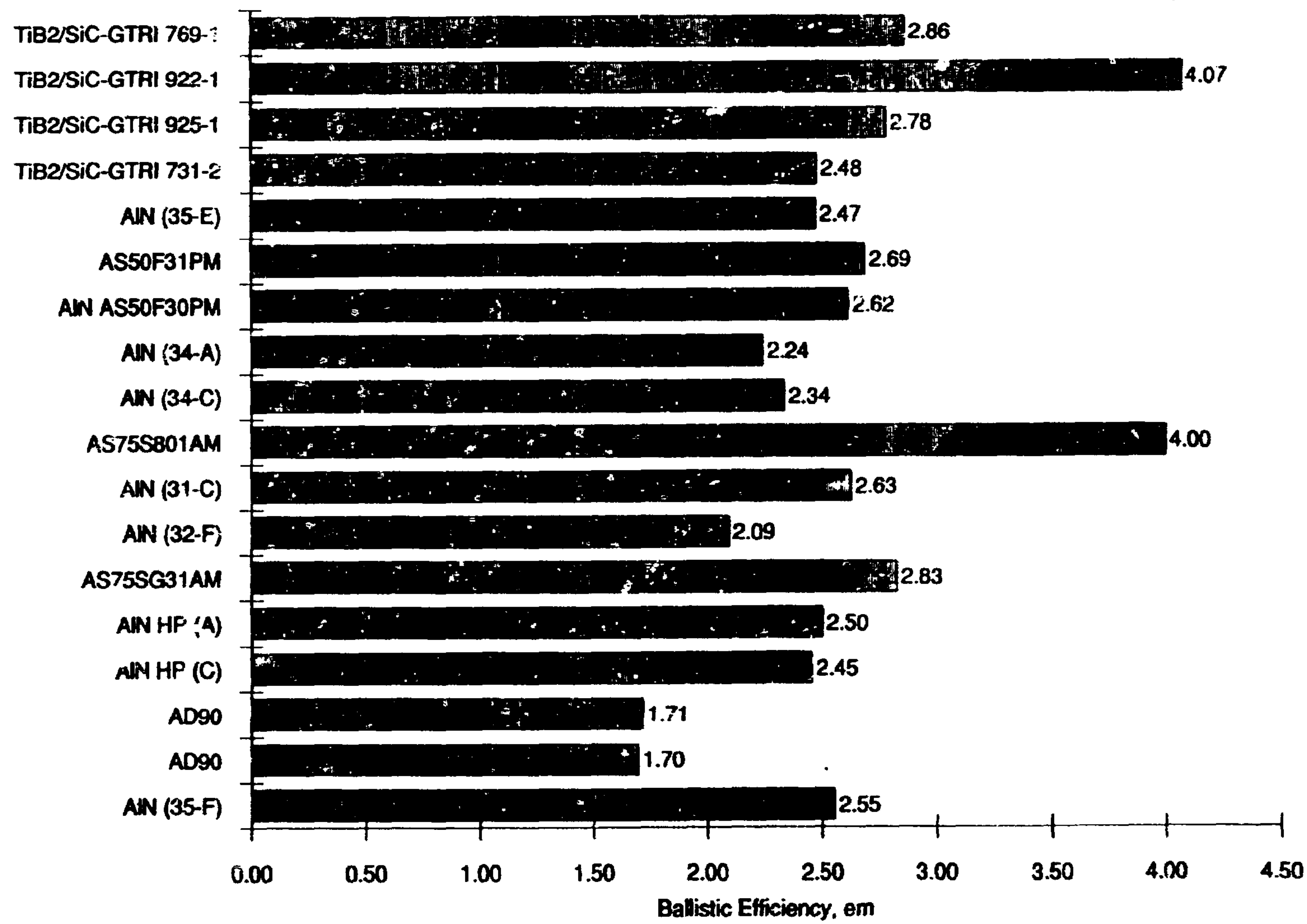

Figure 3.10. Ballistic Efficiency of 15 g/cm² Ceramics.

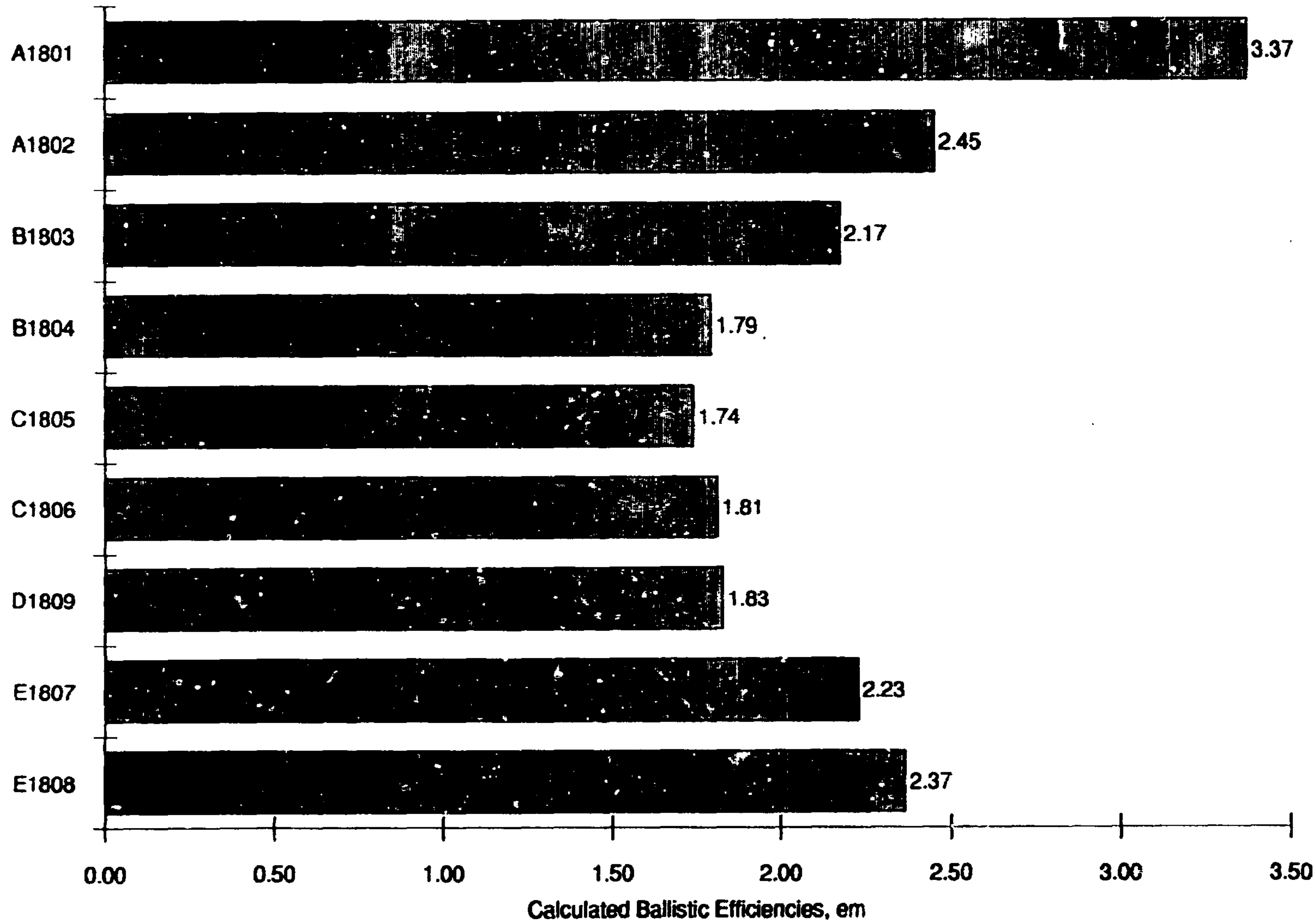

Figure 3.11. SWRI Calculated Ballistic Efficiencies for Areal Density = 15 g/cm² Ceramics.

SECTION 3
REFERENCES

1. D. Yaziv, G. Rosenberg, and Y. Partom, "Differential Ballistic Efficiency of Applique Armor," 9th Int'l. Ballistic Symp., May 1986.

2. Z. Rosenberg, S. Bless, Y. Yeshurun, and K. Okajima, "A New Definition of Ballistic Efficiency of Brittle Materials Based on the Use of Thick Backing Plates," in Impact Loading and Dynamic Behavior of Materials, ed. C.Y. Chiem, H.D. Kunze, L.W. Meyer, DGM Informationsgesellshaft, 1988.

3. P. Woosley, S. Mariano, and D. Kokidko, "Alternative Test Methodology for Ballistic Performance Ranking of Armor Ceramics," 5th TACOM Armor Coordinating Conf., March 1989.

4. I. Muligard, L. Holmberg, and L.G. Olsson, "An Experimental Method to Compare Ballistic Efficiency of Different Ceramics Against Long Rod Projectiles," 11th Int'l. Ballistics Symp. Burssels, May 1989.

EXHIBIT 1.1

24 AUGUST 1989

DRAFT
SUMMARY OF FINDINGS OF COMMITTEE ON STANDARDIZATION OF THE TEST METHODOLOGY FOR BALLISTIC PERFORMANCE OF CERAMICS AND CERMETS

By:
Stephan J. Bless

University of Dayton Research Institute

HISTORY

In recent years several different laboratories in the U.S., Israel, and Sweden have developed special screening tests for armor ceramics. These tests differ from V_{50} tests, in that their purpose is to compare ceramics, not to develop engineering design data for ceramic armors. These tests are all versions of the thick backing plate technique, sketched in Figure 1. In the experiments, an overmatching projectile penetrates a ceramic tile and enters a metal substrate. The penetration in the substrate is used to calculate various figures of merit for the test ceramic.

Referring to Figure 1, we define W_C as the areal density of the ceramic, W_R as the penetrated weight (thickness x density) of the substrate, and W_{REF} as the penetration in the substrate when no tile is present. Figure 2 is a graph of the trend usually observed in experiments. The differential efficiency of the ceramic relative to the substrate is

$$\Delta e = \frac{W_{REF} - W_R}{W_C}$$

Table 1 is a resumé of ceramic screening experiments that have been reported.

TABLE I
TECHNIQUES USED TO SCREEN CERAMICS

Projectile	Tile Shape	Tile Width (mm)	Tile Thickness (mm)	Side Confinement	Coverplate	Backplate	Performance Meas.	References	v (km/s)	Year
LRP L/D = 15	Round	75 to 100	35 mm typ	Steel	40 mm steel with hole + plastic	HB 300 steel	Δe_c	1	1.3 to 1.8	1989
65 g 91W L/D = 10 LRP	Square	150	6.4 to 50	Steel	None	RHA	W_R	4	1.5	1989
L/D = 4 W	Square	???	???	Steel	None	Hard Steel	W_c^0 Note 4	7	? to 3	1989
21 g LRP L/D = 13	Square	75 mm	6.4 to 50	Aluminum	Aluminum	6061T6 Aluminum	Δe, W_c^0	8	1 to 3	1989
65 g Rod	Square	75 mm	Various	Steel	Steel	Steel	Δe	11	1.5	1989
1.2 g L/D = 23 W	Round	50 mm	Various	Steel	Steel with hole	Steel	u	9	1.5	1988
AP Bullets	Square	Various	Various	None	None	Various Aluminum	Δe_1	2,3	typ 0.9	1987
Various	Square	75 mm	9	None	None	6061T6	Note 1	5	1.0 to 3	1987
66 g L/D = 10 W2	Round	50 mm	Various	Aluminum	None	Aluminum	u Note 3	10	1.5	1987
AP Bullets	NA	NA	NA	NA	NA	RHA	DEF Note 2	6	Various	1986

Note 1 $e = 1 - \frac{W_R - W_C}{W_{REF}}$.

Note 2 DEF defined as Δe, but used for standoff applique armor.

Note 3 u_0 = penetration rate.

Note 4 W_C^0 = weight ceramic to just make $W_R = 0$.

A meeting was held 18 April 1989 to discuss issues concerning a standard screening test for armor ceramics. Table 2 lists the attendees at this meeting. Stephan Bless served as Chairman.

On 5 June 1989 Charlie Anderson released a draft test procedure. Copies of the draft were circulated to attendees at the 5 June 1989 meeting for their comments.

Other individuals were also invited by Dr. Bless to contribute to the discussions. These are listed in Table 2A.

Comments were requested from everyone listed in Table 2 and 2A. Written comments were received from S.C. Chou (AMTL), W. Blumenthal (LANL), and G. Hauver (BRL). Oral comments were received from W. Gooch (BRL), C. Cline (LLNL), R. Hoffman (Dow), and I. Ahmad (ARO). My conclusions based on these comments are summarized below. Letters from S. Chou, W. Blumenthal, and G. Hauver are included as appendicies.

1. GENERAL

The techniques proposed by SwRI are okay if testing must begin at once. However, they should not be adopted as the final standard test protocol until several outstanding issues are settled.

It is very likely that relative performance of armor ceramics is threat and application dependent. For example, apparently many ceramics which perform adequately for brittle steel bullets are ineffective against W penetrators. Furthermore, some ceramics perform well with relatively little confinement, whereas other may benefit greatly from confinement. The goal of the present test procedure is to screen ceramics for LRP protection. Wider applicability should not be claimed. The test procedures developed here may well serve as the kernel for a more complete protocol to evaluate ceramics for a wider range of applications.

2. FORMAT

The scope of the test protocol should explicitly reference past work (see Table 1). The assumptions discussed in the draft document are not necessary. W. Blumenthal, in his letters, has provided several suggestions for how to improve the background section of the document.

The test protocol should be consistent with ASTM standards. ASTM procedures should be referenced whenever possible. ASTM format should be employed. Interaction with ASTM C-28.01 Committee on Mechanical Properties would be desirable.

3. TILE SPECIFICATIONS

There is much concern about tile dimension. Studies with quarter-scale rods have shown decreased performance in tile < 4 inches. Other studies indicate little or no loss of performance in small tiles that are stiffly confined.

Since the screening test is designed to be an inexpensive technique for QA or new tile evaluation, the sample size should be kept small. We think that the 4 inch tiles proposed by SwRI are adequate as long as they are snugly confined in steel.

Chamfer on the tile is not necessary. Surface finish should be per MTL specs or else specifically noted.

Ceramic characterization should not be the burden of the screening agency, except perhaps for sound speed and density, which are readily obtained with instrumentation available in most testing laboratories. However, the test report should include as much data as are available about the tiles. Table 3 contains a list of desirable information.

4. CONFINEMENT STRUCTURE

There is a concensus that a steel backplate is best. However, the backplate should be 4340 HRC 27 ± 2. A softer material provides better resolution. It is also characteristic of bulk armor steel. The DARPA-mandated hardness of HRC 37 is program specific, and not advisable.

There is no concensus about cover plates. Reference to Table 1 shows wide variations in current practice. Some ceramics have been observed to perform worse with cover plates. We are unaware of demonstrated improved performance with cover plates, except where interface dwell occurs. Interface dwell seems to be a geometric effect that is not of interest to ceramic screening experiments. Therefore, we propose that no cover plate be used.

TABLE 3
DESIRABLE INFORMATION ABOUT CERAMICS

1. Manufacturer, including batch, powder lot, process, applicable specifications.
2. Composition.
3. Microstructure (including photographs of grain structure, if available).
4. Mechanical properties, density, sound speed, Young's modulus, Poisson's ratio, Knoop hardness (1000 g load).
5. Physical appearance (color, finish).
6. Porosity.

The procedure for radiographing the substrate should spell out a fiducial system. The section should be radiographed twice, with adjacent sides against the film, to correct for curved penetration channels.

5. PROJECTILE

For screening, all that matters is consistency and that the rod significantly overmatch the target. However, several investigators have found it advantages to use W_c^0 as a figure of merit for ceramics. If the projectile is a 65 g quarter-scale rod, Then W_c^0 is probably the optimum size tile to use in a stand-alone armor. This is a valuable side benefit of screening experiments. Therefore, we recommend that the penetrator actually be a generic quarter-scale rod.

6. TARGET FIXTURE

The test procedure should include design of the target fixture. This should be robust and reversible. BRL and UDRI, for example, have developed standard target mounting procedures.

7. NEED FOR MATERIAL STANDARDIZATION

One approach to testing is to strictly specify all aspects of the test procedure so that residual penetration data taken in different laboratories can be directly compared. We suggest a less rigorous approach in which relative performance parameters are measured.

Each apparatus should be calibrated by measuring W_R as a function of W_c with a standard ceramic. We propose armor-grade Coors AD998 (CAP 3) for this purpose. The ceramics may be compared to the "standard" by computing

$$e_R = \frac{W_c \text{ (for CAP 3)}}{W_c \text{ (test ceramic)}} \quad \text{for same } W_R.$$

The value of e_R would include error brackets representing the uncertainity in the W_R measurements.

Whatever figure of merit is adjusted, the reference data must include the effects of small excursions in velocity from the nominal value.

8. RECOMMENDED TEST PROGRAM

We strongly recommend that ARO sponsor a test program to clarify the importance of certain test parameters before the test procedure is finalized. Table 4 lists the components of the test program.

TABLE 2
ATTENDEES AT 18 APRIL 1989 MEETING
UNIVERSITY OF DAYTON RESEARCH INSTITUTE

Dr. Marv Alme	RDA	(703) 684-0333
Dr. William Blumenthal	LANL	(505) 667-6972
George Roth	UDRI	(513) 229-3812
Patrick Woolsey	AMTL	(617) 923-5187
Stephen Mariano	AMTL	(617) 923-5233
Ron Hoffman	DOW	(517) 638-7313
George Hauver	BRL	(301) 278-6052
Dr. Charles Anderson	SwRI	(512) 522-2313
Dr. Kalisam Iyer	ARO	(919) 549-0641
Dr. Iqbal Ahmad	ARO	(919) 549-0641
Andrew Crowson	ARO	(919) 549-0641
Dr. George Mayer	IDA	(703) 578-2864
Dr. N. Singh Brar	UDRI	(513) 229-3546
Dr. Stephan Bless	UDRI	(513) 229-3546

TABLE 2A
ADDITIONAL INDIVIDUALS INVITED TO
REVIEW SCREENING PROCEDURES

Dr. Marc Adams	JPL	(818) 354-3031
Dr. Carl Cline	LLNL	(505) 667-6972
William Gooch	BRL	(301) 278-6052

TABLE 4
EXPERIMENTAL STUDIES NEEDED TO HELP DEVELOP
SCREENING PROCEDURE
All tests conducted with armor-grade alumina and B_4C.

	SUBJECT	APPROACH
1	Tile size study.	Tile aspect ratios of 3:1, 4:1, and 6:1. Do tests with steel lateral confinement and no lateral confinement.
2	Cover plate study.	Tests with mild steel and hard steel. Cover plate thickness 0, 1, and 4 projectile calibers. Cover plate in intimate contact or separated by 0.5 caliber elastomer.
3	Tile thickness study.	Test tiles in thicknesses of 1 to 10 calibers. Vary rod L/D to maintain good resolution.
4	Shape study.	Compare square and round tiles in square and round containment blocks.
5	Study effect of filler material.	If study 1 shows confinement effects, then test tight tiles and tiles with 0.5 mm gaps filled with epoxy or Belzone.
6	Determine W_R statistics.	Shoot a fixed ceramic tile at least six times and compute the variance of the W_R measurement.
7	Determination of V_{50} correlation.	The tiles examined in tests 1 and 3 should be used in stand-alone armor targets with steel and GRP substrates. V_{50} values should be determined and compared with screening ranking.

REFERENCES

1. I. Mellgard, L. Holmberg, and L.G. Olsson, "An Experimental Method to Compare the Ballistic Efficiencies of Different Ceramics Against Long Rod Projectiles," 11th International Ballistic Symposium, Brussels, May 1989.

2. Z. Rosenberg, S. Bless, Y. Yeshurun, and K. Okajima, "A New Definition of Ballistic efficiency of Brittle Materials Based on Use of Thick Backing Plates," Impact Loading and Dynamics Behavior of Materials, C.Y. Chiem, H-D Kunze, L.W. Meyer, eds., Informationgesellschaft Verlag, pp 491-498, 1988.

3. Z. Rosenberg and Y. Yeshurun, "An Empirical Relation to the Ballistic Efficiency of Ceramic Tiles and Their Effective Compressive Strength, " 10th International Symp. Ballistics, October 1987.

4. S. Mariano and P. Woolsey, "Alternative Test Method for Ballistic Performance Ranking of Armor Ceramics," Fifth TACOM Armor Coordinating Conference, Monterey, CA, 7-9 March 1989.

5. S. Bless, Z. Rosenberg, and B. Yoon, "Hypervelocity Penetration of Ceramics, Int. J. Impact Eng. 5:165-171, 1987.

6. D. Yaziv, G. Rosenberg, and Y. Partom, "Differential Ballistic Efficiency of Applique Armor," 9th Int'l. Ballistics Symp. Paper, TBZ, May 1986.

7. C. Cline, Private communication, 1989.

8. S. Bless, J. Gonzalez, N. Brar, M. Alme, and C. Terry, "Ceramic Armor Design Study," Fifth TACOM Armor Coordinating Conference, Monterey, CA, 7-9 March 1989, and S. Bless and M. Alme, "Hypervelocity Penetration of Ceramic Targets by Long Rods," Hypervelocity Impact Symp., San Antonio, TX, December 1989.

9. G. Hauver, Presentation at DARPA Impact Physics Group Thids Quarterly Review, 10-11 February 1988.

10. M.L. Wilkins, "Penetration Studies of Ceramic Armor Materials," CONFIDENTIAL, UCID-21183, September 1987.

11. W. Gooch, private communication, 1989.

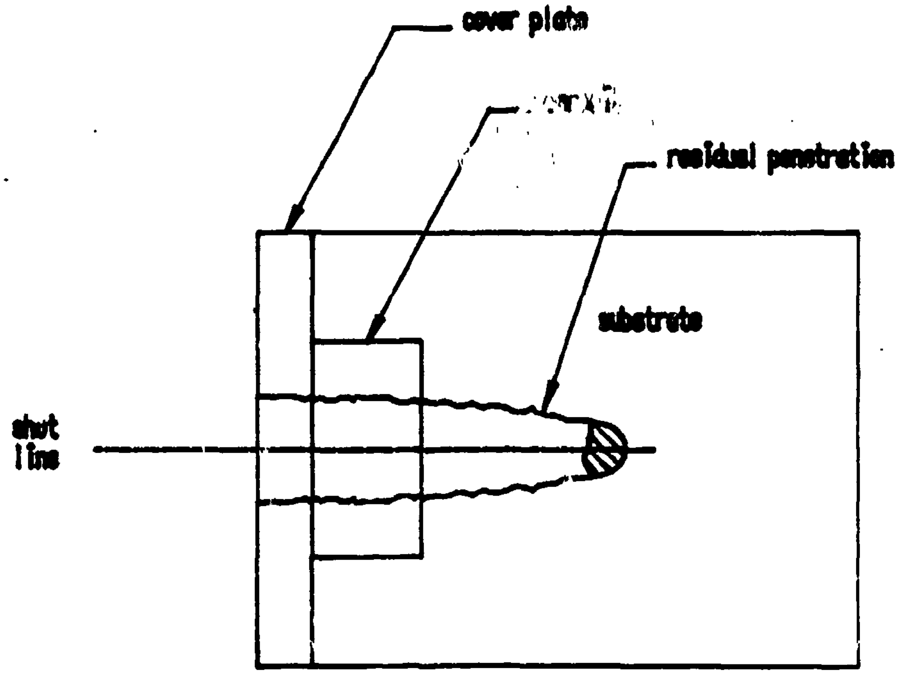

TEST

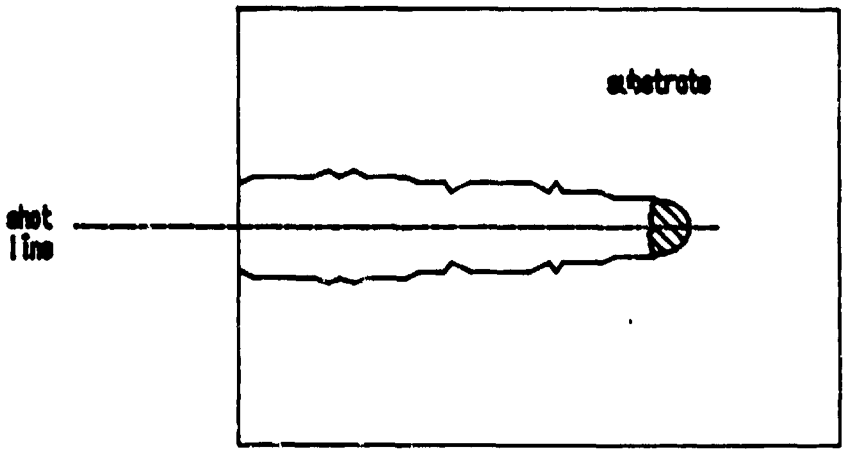

REFERENCE

g. 1

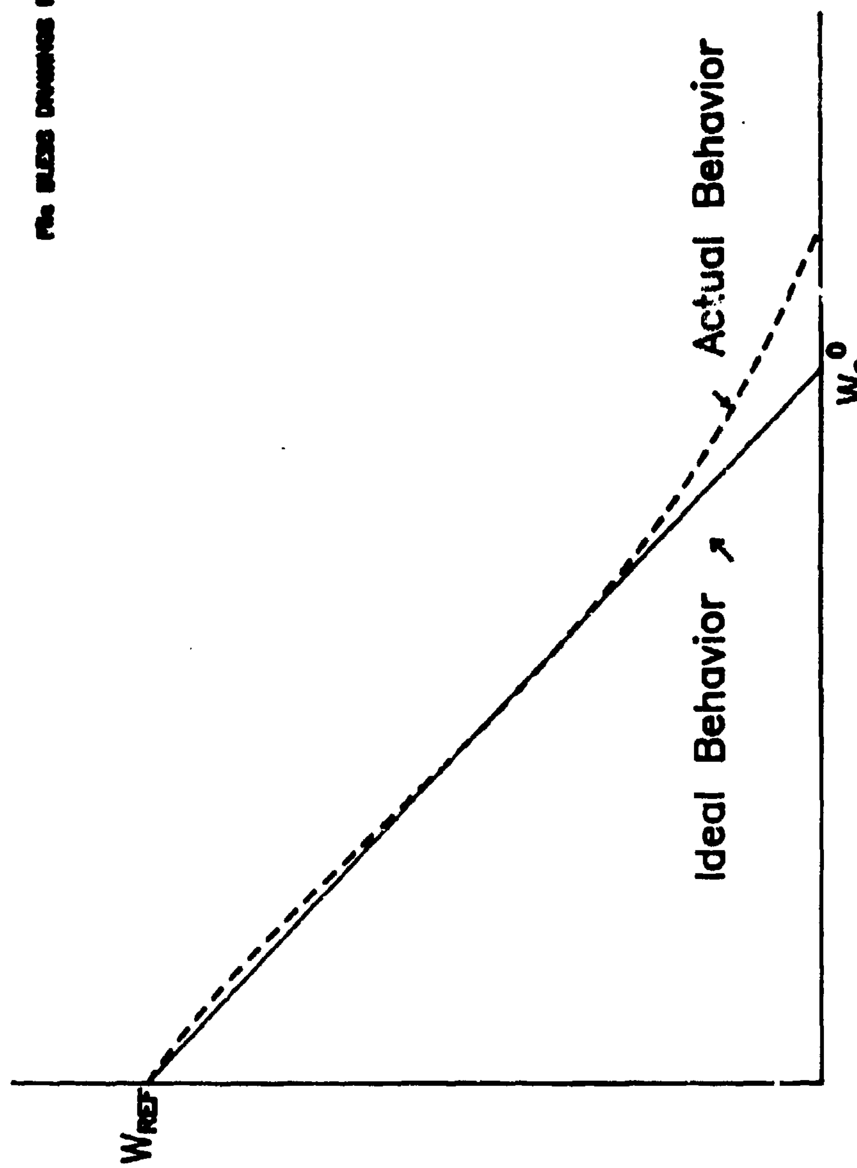
Actual Behavior
Ideal Behavior
W_{REF}
W_c^0